0 0 0 0 4 8 0 2 0 2 2

UC-34d

LBL-6472 c.1
Preprint

To be Submitted for Publication

$\pi^- p$ CHARGE-EXCHANGE DATA AMPLITUDE ZEROS FROM A BARRELET ANALYSIS BETWEEN 1.4 AND 2.3 GeV

D. M. Chew

RECEIVED
JUL 7 1978
LIBRARY AND
DOCUMENTS SECTION

October 1977

Prepared for the U. S. Department of Energy
under Contract W-7405-ENG-48

For Reference

Not to be taken from this room

LAWRENCE BERKELEY LABORATORY
UNIVERSITY OF CALIFORNIA
BERKELEY

LBL-6472 c.1

DISCLAIMER

This document was prepared as an account of work sponsored by the United States Government. While this document is believed to contain correct information, neither the United States Government nor any agency thereof, nor the Regents of the University of California, nor any of their employees, makes any warranty, express or implied, or assumes any legal responsibility for the accuracy, completeness, or usefulness of any information, apparatus, product, or process disclosed, or represents that its use would not infringe privately owned rights. Reference herein to any specific commercial product, process, or service by its trade name, trademark, manufacturer, or otherwise, does not necessarily constitute or imply its endorsement, recommendation, or favoring by the United States Government or any agency thereof, or the Regents of the University of California. The views and opinions of authors expressed herein do not necessarily state or reflect those of the United States Government or any agency thereof or the Regents of the University of California.

0 0 0 0 4 8 0 2 6 2 3

(To be submitted for publication) LBL-6472

$\pi^- p$ CHARGE-EXCHANGE DATA AMPLITUDE ZEROS FROM A BARRELET ANALYSIS BETWEEN 1.4 AND 2.3 GeV

D. M. Chew†

Lawrence Berkeley Laboratory
University of California
Berkeley, CA 94720

October 1977

ABSTRACT

Using the available scattering and polarization pion-nucleon charge-exchange data, we have performed a Barrelet moment analysis between 1.4 and 2.3 GeV. The method allows us to identify and discard data with important systematic error. Above 1.5 GeV, 10 zeros are unambiguously required in order to represent the retained data. An attempt is made to resolve the discrete ambiguity and to obtain the location of amplitude zeros close to the physical region.

*Prepared for the U. S. Energy Research and Development Administration under Contract W-7405-ENG-48

†On leave from the University of Paris VI, Paris, France

I. Introduction

Data on the charge-exchange reaction [1,2]

$$\pi^- p \to \pi^0 n \tag{1}$$

constitute an important supplement to elastic $\pi^{\pm}p$ data, since isospin invariance relates the charge-exchange amplitude to the difference of the two elastic amplitudes. The recent availability of accurate charge-exchange data makes it possible to check amplitude analyses that have been based on elastic data alone.[3] These checks have revealed alarming discrepancies[4]. Either the recent charge-exchange measurements are grossly in error, or currently accepted elastic amplitudes based on partial-wave analysis possess serious deficiencies. As part of a Barrelet-zero approach to πN amplitude analysis[5,6] which we hope will lead to more reliable conclusions than have been reached by the partial-wave route, we lay the groundwork in this paper for a direct determination of the charge-exchange amplitude.

For reasons explained elsewhere, amplitude analysis through Barrelet moments and Barrelet zeros[7] is less subjective than conventional partial-wave analysis in conjunction with least-square polynomial fitting. The Barrelet method furthermore, by objectively generating moments from individual experiments, is capable of revealing systematic error.[8] In this paper, we report the results of Barrelet-moment analysis for available charge-exchange data in the interval $.6 < P_{lab} < 2.5$ GeV/c ($1.4 < E_{c.m.} < 2.3$ GeV)*. After eliminating certain data which have large statistical errors or which our results suggest possess systematic error larger than the stated statistical error, we determine the trajectories of the Barrelet-zeros that come sufficiently close to the

*For reasons to be explained we analyze only experiments with data from at least 20 different angles at a given energy.

physical region to be detected. The discrete ambiguity is handled by the method that has been used earlier for elastic data[5,6].

We do not discuss in this paper the determination of the charge-exchange amplitude in terms of zeros, or the comparison with the difference of $\pi^- p$ and $\pi^+ p$ elastic amplitudes. These steps will be reported in a later paper.

II. Method of Analysis

Barrelet developed his method[7] for use with individual experiments that each cover a finite portion of the physical angular interval $a < \cos\theta < b$. In this interval, the differential cross section is represented by a superposition of orthonormal pseudopolynomials $p_\ell(\cos\theta)$:

$$\frac{d\sigma}{d\Omega} \simeq \sum_{\ell=0}^{\ell=N_1} A_\ell p_\ell(\cos\theta) \tag{1}$$

The pseudopolynomials are defined with respect to a weighting norm $n_p(\cos\theta)$ such that

$$\int_a^b d(\cos\theta)\ p_\ell(\cos\theta)\ p_{\ell'}(\cos\theta)\ n_p(\cos\theta) = \delta_{\ell\ell'} \tag{2}$$

the moments A_ℓ being calculated from the formula

$$A_\ell = \int_a^b \frac{d\sigma}{d\Omega}(\cos\theta)\ p_\ell(\cos\theta)\ n_p(\cos\theta)\ d(\cos\theta) \tag{3}$$

With data sufficiently dense in $\cos\theta$, the latter quadrature, when carried out with care, allows translation of the statistical error on individual data points into statistical errors for the moments A_ℓ. Barrelet chooses the truncation point N_1 of the polynomial expansion on the basis that A_ℓ is theoretically expected to tend smoothly toward zero for ℓ sufficiently large*. As soon as the error in the moments begins to overlap zero, Barrelet terminates the expansion in Eq. (1) ;

* If R is the radius of the ellipse (in the $z=\cos\theta$ plane) passing through the first singularity, then the coefficients A_ℓ have an asymptotic behavior like $(1/R)^\ell$ as $\ell \to \infty$.

to go futher is statistically meaningless. The parameter N_1 is determined by the data, not guessed. For spin 0-spin 1/2 elastic scattering where the polarization P can be measured, one may make a similar analysis of $P \frac{d\sigma}{d\Omega}$, leading to a second set of moments B_ℓ with $\ell < N_2$.

The weighting norm is to be chosen so as to give comparable weight to all data points in the calculation of the moments[8]. In the case of the CEX data, we take n_p equal to 1. A major advantage of the Barrelet method of data analysis is that Barrelet's truncation points N_1 and N_2 are objectively fixed by the statistical errors. The polynomial fit arrived at thorugh Formulas (1) and (3) contains all the information in the data. It takes into account information due to either low statistics (which reflect into the errors on the moments) or systematic errors larger than the statistical errors (which affect the asymptotic behaviour of the moments), as explained in the following section*.

III. Selection of data

We have considered the results of all charge-exchange differential cross-section experiments where measurements were made for at least 20 different angles (at each energy). Columns 2,4 and 5 of Table I list the characteristics of each of 41 different experiments. A sequence of Barrelet moments was determined for each experiment[9.10] according to the prescription of Section II above, the sequence being terminated when two successive moments both have statistical errors that overlap zero. For data where systematic error is smaller than the statistical error, the upper limit N_1 so defined (listed in column 6) coincides with the maximum-order moment that is significant. At a given energy, the relative statistical accuracy of different experiments is measured by N_1, so we may use low relative values of this parameter as an objective basis for eliminating data. This criterion leads us to discard

* The last point constitutes an important advantage over a least square fit method which has no way of distinguishing between correctly measured points and those affected by systematic errors.

immediately the results from C67, B64 and C69.*[1]

Although Barrelet moment analysis was not designed to deal with systematic error, we may use it to identify experiments that contain significant systemaatic abberations--as we now explain. For data where the error is predominantly statistical one expects the goodness of fit achieved by the Barrelet polynomial representation of Formula (1) to increase with the order of the polynomial up to the limit N_1. The expansion coefficients (moments) are theoretically supposed to decrease exponentially (see footnote on previous page), so we expect to see the chi-squared per data point fall smoothly to the neighborhood of 1 as the polynomial order approaches N_1; thereafter the goodness of fit should not change significantly. Polynomials of order higher than N_1 are not physically meaningful--corresponding merely to statistical fluctuations in the data-- but their inclusion should not suddenly spoil the goodness of overall fit.

Suppose, on the other hand, that there is a small proportion of data points with large systematic error. These points are (more or less) ignored by moments of low order but seriously influence the value of appropriately high-order moments. Inclusion of such high-order moments may upset the overall goodness of fit. Systematic error is thus signaled by a chi-squared per data point that rises (or fluctuates) significantly in the neighborhood of N_1 <u>after</u> a minimum has been achieved. An even more obvious signal is the absence of any smooth tendency for the chi-squared per point to approach the neighborhood of 1.

Figure 1 shows the chi-squared per data point as a function of polynomial order at each B76 and N72 energy. We are led by such considerations to believe that serious systematic errors exist in the N72 data at all of the

*The 2 highest energies could be considered from a statistical point of view but would have to be disregarded because of our finding systematic errors larger than the statistical errors. (See below)

six different energies where measurements were made (Fig. 1a). As explained later, the maximum statistically significant order is ~ 10. We do not include any of the N72 data in the remainder of our analysis. Similar considerations lead us to discard in principle B76 data at four neighboring energies, P_{Lab} = 0.776, 0.825, 0.974 and 1.027 GeV/c (Figs. 1b, and 1c for detail) and the last 2 energies of C69. The degree of disagreement between the N72 and B76 data is indicated in Fig. 2 where we compare at the same energy the polynomial representation of B76 (see Table II) with the data of N72 and its polynomial representations of order 6 (a) and 10 (b,c,d).

Some check on our selection of data can be achieved by comparing two independent pieces of information on forward and backward differential cross sections. Table II lists the chi-squared values plotted in Figs. 1b and 1c and for each polynomial order gives our extrapolation of the differential cross section to 0° and 180° of B76. These extrapolations for N_1=10 are plotted in Figs. 3a and 3b, the indicated error being the largest deviation between the N_1=10 extrapolation and the extrapolation for any other order whose chi-squared value differs from that for N_1 = 10 by less than one unit. We show in Fig. 3a the forward differential cross section as determined from $\pi^- p$ total cross sections and dispersion relations.[11] A uniform shift of about 10% in our extrapolated values would bring agreement. If the problem is only a matter of overall normalization of the scattering data, there will be no effect on the positions of Barrelet zeros. Direct high-precision measurements of $d\sigma/d\Omega$ at 180° have been made[12] and are compared with our extrapolations in Fig. 3b. A significant discrepancy with D75 appears at $P_{lab} \sim 0.700$ GeV/c, but we understand[13] that the authors of D75 now believe their measurement may have contained substantial systematic error. Above 1.5 GeV/c we find ourselves in agreement with A68 and K72. No direct data exist for 1.0 GeV/c < P_{lab} < 1.5 GeV/c

with which to compare our extrapolations.

Table III lists the available polarization data-- two experiments, B76 and S74, being included. Superficial comparison of the data immediately reveals an energy, corresponding to P_{lab} = 1.03 GeV/c, where the two experiments qualitatively disagree in the backward direction, B76 giving a positive polarization and S74 a negative. Because backward direction polarization is here varying rapidly with energy (See Figs. 6- 25 of the B76 data), an error in the beam momentum of one of the experiments by 20 or 30 MeV could account for the discrepancy.

Momentarily ignoring this difficulty, it is straightforward to make a Barrelet moment analysis of $P \frac{d\sigma}{d\Omega}$ at those energies where both P and $\frac{d\sigma}{d\Omega}$ data have been taken and to examine goodness of fit as a function of polynomial order, exactly as we did above for $\frac{d\sigma}{d\Omega}$. However, for Barrelet-zero determination of the amplitude F (s,w) it is necessary to consider the experimental quantity $\Sigma(w)$, where $w=e^{i\theta}$

and

$$\Sigma(w) = \Sigma^{+} = \frac{d\sigma}{d\Omega}(1+P), \quad 0 < \theta < \pi \tag{4}$$

$$\Sigma(w) = \Sigma^{-} = \frac{d\sigma}{d\Omega}(1-P), \quad \pi < \theta < 2\pi \tag{5}$$

so we shall treat polarization data via Barrelet's moment analysis of $\Sigma(w)$ with respect to pseudopolynomials in the variable w[7]. (Polynomials in $\cos\theta$ are pseudopolynomials in w.) The maximum significant order N is set by the smaller of the two separate truncation points N_1, N_2. This maximum order will limit the number of zeros that can be determined from the data (and eventually the number of different partial waves). Because polarization

measurements are less accurate than differential cross sections, it is generally N_2 that sets the limit, i.e., $N=N_2$. The angular interval, furthermore, is the smaller of the intervals covered in the separate measurements of P and $\frac{d\sigma}{d\Omega}$.

Our approach then is to combine data on P and $\frac{d\sigma}{d\Omega}$ so as to generate moments of $\Sigma(w)$ and corresponding pseudopolynomial representations of $\Sigma^+(w)$ and $\Sigma^-(w)$ $(= \Sigma^+(\bar{w}))$. Representations of $\frac{d\sigma}{d\Omega}$ and P may be obtained from

$$\frac{d\sigma}{d\Omega} = 1/2\ (\Sigma^+ + \Sigma^-) \tag{6}$$

$$P = \frac{\Sigma^+ - \Sigma^-}{\Sigma^+ + \Sigma^-} \tag{7}$$

Because of the linearity of the relations (4), (5) and (6), the polynomial representation of $\frac{d\sigma}{d\Omega}$ is affected by the polarization data only to the extent that the angular interval may be contracted and the value of N reduced.

In the absence of systematic errors, the behavior of the goodness of fit (chi-squared per point) for <u>both</u> $\frac{d\sigma}{d\Omega}$ and P should be as described above for $\frac{d\sigma}{d\Omega}$. Figure 4 shows the chi-squared per point as a function of polynomial order N for the B76 scattering and polarization data within a common angular interval. Notice--in Fig. 4(a)--that the $\frac{d\sigma}{d\Omega}$ behavior is similar to that of Fig. 1(b)--the same four neighboring energies exhibiting evidence of a systematic error larger than the statistical error. The polarization chi-squared per point in Fig. 4(b), reveals no such evidence.

The degree of disagreement between B76 and S74 polarization measurements is indicated in Fig. 5 where we compare our different polynomial approximations to S74 with the closest-energy (within 10 MeV) order - 10 polynomial approximation to B76. Due to the fact that (1) we find no evidence for systematic

error in the B76 polarization measurements, (2) the polarization statistical errors are larger for S74 than B76, (3) the angular interval covered is smaller in S74 than in B76, we henceforth disregard the S74 polarization data. The choice N=10 will now be discussed.

IV. Determination of the number of stable zeros:

It turns out, both from examination of Tables I and III and from the original Barrelet criterion, that N varies between 7 and 13 at the different energies under consideration. At the highest energies the variation is between 8 and 12. Changing N by 1 or 2 units at a given energy does not strongly alter the goodness of the polynomial fit* (see Fig. 4), but there may be an important alteration in the location of some of the zeros of $\Sigma(w)$. A stable zero is one whose position does not drastically change when the order of the polynomial is changed. It was shown by Barrelet that stable zeros are near the physical region (the unit circle in the complex w plane), so instability means a large uncertainty in the zero's position.

Analysis of the πN elastic scattering [5-7] has confirmed the theoretically-expected smooth behavior of the position of zeros as a function of energy, especially in intervals free from strong and sharp resonances. Zeros do not suddenly appear or disappear**. It has furthermore been shown that zeros occur in approximately complex-conjugate pairs, so one expects the total number of nearby zeros to be even. We have consequently examined the position of zeros for N=6, 8, 10 and 12 at each energy and looked for smoothness of position variation. The following results have emerged:

a) At the two lowest energies, P_{lab} = 0.618 and 0.675 GeV/c, the 6th-order polynomial has relatively stable roots corresponding roughly to the 6 nearby zeros labeled (A,H), (C,B), (E,F) in Table IV and gives an

---

* At least for the energies of B76 which do not manifest large systematic errors.

** However they may "jump" (i.e. move very rapidly away from the physical region) in an energy region dominated by a sharp resonance (see paragraph VII below).

acceptable value of chi-squared per point (1.85 and 3.25 respectively versus 0.87 and 2.64 for the 10th order polynomial at the same energies).

b) At the next energy (p_{lab} = 0.724 GeV/c), however, and most energies within our range, two additional pairs of stable zeros (within the disc of polynomial convergence) need to be accommodated. They are labeled (D,I) and G,J).

Therefore, the minimum N that can handle the entire energy interval is N=10. Using N=12 does not anywhere significantly improve the goodness of the polynomial representation. The two extra zeros that appear when N is changed from 10 to 12 seem to represent a statistically meaningless "doubling" of two zeros already present. The pattern of doubling shows no consistency as the energy varies. Consequently, since both conditions--stability of the zeros at most energies within our energy range and a consistent pattern in the position of the zeros--are realized for N=10 (see Fig. 26, the labels of Table IV being displayed at p_{lab} = 1.438 GeV/c) we have chosen to work uniformly with this value of N. Ten zeros are correspondingly deduced at each energy. At some energies, less than ten zeros are "stable" in the sense of Barrelet, this fact being exhibited by the failure of one or more zero positions to be securely (within errors*) located inside the disc of convergence. (Even more accurate data are needed for a better determination of their position, as can be observed from the data of Figs. 5 through 25, at the value of cosθ Re z_i given in Table IV.) ⟶

---

*Should the zeros drawn inside the unit circle be positioned outside, the error bars would be enlarged by a factor $|w|^{-2}$ (See Ref. 10).

The fact that already at p_{lab} = 0.724 GeV/c all ten zeros are unambiguously stable is remarkable considering that in the available data [5,6] for π^+p elastic scattering , ten zeros were not required until p_{lab} = 1.450 GeV.c. Figures 6 through 25 show the N=10 polynomial representations of the B76 data, the corresponding chi-squared per data point being given by the dotted line on Fig. 4a.

V. Zero trajectories

At each energy we have determined 11 moments of $\Sigma(w)$ and converted this information into the positions of ten zeros in the complex w plane. There is the usual discrete ambiguity between the location w_i and $\bar{w}_i^{-1}$, to which we devote attention in the following sections. In Fig. 26 we have presented our results at each energy, with the convention that all zeros lie outside the unit circle except for the 2 furthest ones from the physical regions (which would have to be drawn too far out of the plot). The inside boundary of the disc of convergence of the polynomial expansion is indicated, allowing identification of the nearby stable zeros.

By comparing the positions of zeros at neighboring energies, where the relative displacements are moderate, it is possible to construct trajectories w_i in the complex w plane.

The continuity of individual trajectories is nicely displayed by plotting Re t_i vs. $\sqrt{s}$. The complete set of 10 trajectories is thus shown in Fig. 27 and then two at a time (Figs. 28 through 32) with errors. The five trajectories labeled A,C,E,G,I represent zeros of Σ^- (corresponding to polarization maxima) while those labeled B,D, F, H, J represent zeros of Σ^+(polarization

*The radius of the outside boundary is the inverse of the radius of the inside boundary.

minima). Note that for such a plot the discrete ambiguity is irrelevant. On the same Fig.s 28 through 32 are displayed also the ten trajectories in the complex w-plane, with the errors for $|w_i| > 1$. The two trajectories (D and I) that wander farthest from the physical region are poorly determined, but at certain energies even these zeros come close enough to produce extreme polarization at $\cos\theta = \mathrm{Re}\, z_i$. Table IV lists the positions of these 10 zeros (with the convention that they all lie outside the unit circle in the w-plane) in different variables , with the radius of the outside boundary of the convergence disc.

VI. Determination of the critical points

In an effort to resolve the discrete ambiguity, we need first to identify the critical points where trajectories cross the physical region, moving in the w complex plane from inside the unit circle to outside, or vice versa. Because $P = \pm 1$ at a critical point, polarization measurements of high accuracy, closely spaced in energy, can settle this question. In practice, experimental inadequacies leave considerable uncertainty. Fig. 33 plots $|w_i|$ for each zero (assumed outside the unit circle) in the w plane. Critical points occur at energies when the distance goes to zero, i.e., when $|w_i| = 1$. If the statistical error on the measured polarization at such an energy is compatible with $P = \pm 1$, we list the critical point in Table V with 4 stars. If the error bar does not overlap $P = \pm 1$ (or if there are no data at the energy where the polynomial representation of P reaches ± 1), we list the critical point with 2 stars.

Two considerations leave open the door to additional critical points: (1) The possibility of systematic error in polarization normalization. That is, even though the measured polarization or the polynomial representation

thereof fail to reach ± 1, both might do so if $|P|$ were enlarged by, say 10%. To explore this possibility we have allowed 10% variation in the normalization of the B76 polarization data and repeated our analysis. Critical points thereby found are assigned 3 stars. When found close to ("coincident" with) a 4 or 2-star candidate we regard the critical point to be confirmed.*

(2) There is also the possibility that a critical point occurs at an energy between two adjacent measured energies, with such rapid change of polarization that at neither of the measured energies is P compatible with ± 1. It is in fact typically the case that the rate of change of P is unusually high near a critical point. So where we observe a rapid energy variation of P near a polarization extremum we list a one-star possible critical point in Table V. Such critical points evidently have a lower confidence level, but when found in coincidence with 3-star critical points we consider them "confirmed"**

VII. Resolution of the discrete ambiguity

Given the critical points it remains to establish for each trajectory at some particular energy whether it lies inside or outside the unit circle. The discrete ambiguity will thereby be removed at all energies. We here invoke the assumption that there exist individual reasonably-sharp resonances of well-defined angular momentum J and naturality ε, so that near such a resonance the stable zeros are fairly close in position to the 2J-1 zeros of the polynomial $R_{J\varepsilon}(w)$ which are either all inside (ε=+1) or all outside (ε=-1) the unit circle. As the resonance is approached, the "extra" zeros should become unstable. (According to causality considerations, the 2J-1 surviving zeros

---

*A natural assumption, when the analysis yields two or more critical at nearby energies for the same trajectory, is that there is but a single crossing of the physical region. However, near 1 GeV/c for the C trajectory there is an indication from the evidence on 2-, 3-, and 4-star critical points that two separate crossings may occur with a spacing of $\sim$ 50 MeV/c.

**The only non-confirmed 1-star critical points (by any 2-, 3- or 4-star) are A (1;872/1.975 and 2.055/2.267 GeV/c), B(1.438/1.505 and 1.688/1.767 GeV/c) and E(2.055/2.267 GeV/c).

should move in a clockwise sense about the positions of the zeros of $R_{J,\varepsilon}(w)$.

In the neighborhood of the strong 7/2 + resonance near 1900 MeV ($P_{lab} \sim$ 1.5 GeV/c) one does indeed observe(in Fig. 33) that six zeros (3 each in Σ^+ and Σ^-) are close to the physical region while four (2 each in Σ^+ and Σ^-) are substantially further away. Since the zeros of $R_{7/2,+}(w)$ all lie inside the unit circle, it is reasonable to assume at this energy that the six nearest Barrelet zeros also lie inside. What about the remaining four? The next resonance in the same Regge sequence is 11/2 + at 2420 MeV ($P_{lab} \sim 2.6$ GeV/c). It is then plausible that all ten of our trajectories should at that point lie inside the unit circle, close to the physical region. Inspection of Fig. 26 or 33 shows that above P_{lab}=2.2 GeV/c all ten zeros are indeed well inside the strip of convergence. A knowledge of critical points between P_{lab}=2.2 and P_{lab}= 2.6 GeV/c would resolve the discrete ambiguity for all ten trajectories. Lacking such information we still can anchor 6 of the trajectories to the 7/2+ resonance.

The presence of critical points in all four of the nearby zeros near P_{Lab} =1.0 GeV/c (A,B,C, and F) and the general instability here of the remaining zeros is attributed to the proximity of both 5/2+ and 5/2- resonances. The 4 zeros of $R_{5/2,+}$ lie inside the unit circle while those of $R_{5/2,-}$ lie outside.*

Combining our critical points with the 7/2+ anchor, we are able to resolve the discrete ambiguity for the six trajectories (A,H,C,B,E and F) of Table IV, the positions of the zeros heretofore given outside being modified according to the results given in Table V and Fig. 33 (where the part of the trajectories inside the unit circle has been dotted). The uncertainties in this resolution of the discrete ambiguity come mainly from the non-confirmed 1-star critical points: the results could change drastically for B (below 1.438 and/or above

*These critical points explain the difficulty in the measurements of the data around 1.0 GeV/c, because, as observed in the elastic π^+p_+data [5,6], the differential cross section has the deepest minima when P=- 1. (See Figs. 12 and 13).

1.688 GeV/c) and E(above 2.055)

We have tentatively resolved the remaining discrete ambiguity by making the following guesses for the interval between 2.3 and 2.4 GeV about the four trajectories G, I, D, J that are far from the physical region near the Δ 7/2+ resonance near 1.9 GeV: (a) Trajectories G and I, which seem to be heading for the physical region at 2.3 GeV each have one critical point before 2.4 GeV.* (b) Trajectory D, which is still far away at 2.3 GeV, has no critical point before 2.4 GeV (and is therefore assigned the inside location throughout the whole energy range that we have studied), (c) Trajectory I, which has a critical point near 2.3 GeV, has no further critical point before 2.4 GeV. If subsequent experiments indicate otherwise, it will be easy to modify the results.

The zeros under discussion are zeros of the amplitude F(w), which is related to the measured quantity $\Sigma(w)$ by

$$\Sigma(w) = F(w).\ F(\overline{w^{-1}})$$

Consequently, once the positions of nearby zeros in the complex w plane are established, one can place heavy constraints on partial wave analysis and, with information about the modulus and phase at one angle (such as θ=0) can even make an approximate construction of the amplitude[5]. We defer the latter attempt to a subsequent paper.

---

* The same hypothesis has to be made for trajectories B, F and H (unless the 1-star critical point for B around 1.688 GeV/c can be experimentally cancelled) -- even though for none of these trajectories are any signs of these (future) critical points apparent yet at 2.267 GeV/c within the available data.

VIII. Conclusion

We have shown how Barrelet-moment analysis can reveal systematic errors in $\pi^- p$ charge exchange data. Selecting data which does not show symptoms of important systematic error, we have then determined the nearby zeros of the polarized cross section $\Sigma(w)$. The energy interval covered by this data is 1.45 GeV $< \sqrt{s} <$ 2.3 GeV. Within this interval 10 nearby zeros are found, and we give arguments to resolve the discrete ambiguity that arises for the position of each when it is regarded as a zero in the amplitude.

Our analysis depends heavily on identification of critical points and calls attention to the importance of more accurate experiments at those energies where we suggest that critical points occur. Our argument for resolving the discrete ambiguity for all 10 zeros underlines the usefulness of extending the measured energy range all the way up to the Δ 11/2+ resonance.

Acknowledgements

We are very grateful to G. F. Chew for numerous enlightening discussions and his attention to this paper. We thank R. Ely and G. Gidal for their constant encouragement and support. We also wish to acknowledge assistance by R. Kelly, of the Particle Data Group, in providing us with the data necessary for this study.

REFERENCES

1. Scattering data for the reaction $\pi^- p \to \pi^0 n$: The data listed below have been selected on the ground that they present more than 20 data points per energy.

B64 A. Bigi et al. Nuovo Cimento 34, 878 (1964).

B76 R. M. Brown, et al. Rutherford Lab, R1-76093 (1976); Nucl. Phys. B117, 12 (1976).

C67 C. B. Chiu, et al. Phys. Rev. 156, 1415 (1967).

C69 A. S. Carroll, et al. Phys. Rev. 177, 2047 (1969)

N72 J. E. Nelson (Ph.D. Thesis), LBL-1019 (1972).

N73 J. E. Nelson, et al. Phys. Letters 47B, 281 (1973).

For a complete survey of all available data, see: K. H. Augemstein, G. Hohler, E. Pietarinen, H. M. Staudenmaier, Physics Data (Karlsruhe) 1-2 (March 1977).

2. Polarization data for the reaction $\pi^- p \to \pi^0 n$:

B76 R. M. Brown, et al. Rutherford Lab, R1-76093 (1976).

S74 S. R. Shannon (Ph.D. Thesis) LBL-2607 (May 1974);

S. R. Shannon, et al. Phys. Rev. Lett. 33, 237 (1974).

3. (a) S. Almehed and C. Lovelace, Nucl. Phys. B40 (1972) 157.

(b) R. Ayed and P. Bareye (Saclay), Conf. on Elementary Particles, Aix-en-Provence and private communication to the Particle Data Group, (1973).

(c) R. E. Cutkosky, et al. Phys. Rev. Letters 37, 645 (1976).

4. (a) See Refs. N72 and N73 of Ref. (1) above.
(b) See Refs. N72, N73, B76 and S74 of Refs. (1) and (2) above.

(c) R. Kelly (private communication).

5. D. M. Chew and M. Urban LBL-4656 (June 1976); Proceedings of the Topical Conference on Baryon Resonances, Oxford 5-9, July 1976, p. 156.

6. D. M. Chew, E. Barrelet and M. Urban, "Determination of the elastic $\pi^+ p$ zero trajectories from 1.1 to 2.2 GeV center of mass energy", LBL-4644 (under revision and completion with more recent data); for preliminary results see Ref. (5).

7. E. Barrelet, Thesis (1970), Paris (unpublished); Nuovo Cimento 8A, 331 (1972).
8. D. M. Chew, "Data selection through Barrelet moments", LBL-6102 (March 1977).
9. E. Barrelet and M. G. Fouque, Program Moulin, Ecole Polytechnique (1969), completed for the errors by the information from Ref. 10.
10. M. Urban, These de 3^{ieme} Cycle (1973), Paris (unpublished); see also LBL-4809 (feb. 1976) and the Journal de Physique 38 (1977), 1029.
11. G. Holer, H. P. Jakob and F. Kaiser, Tables of pion-Nucleon Forward Amplitudes, TKP 7616, University of Karlsruhe, May 1976.
12. Backward Scattering Data of the Reaction $\pi^- p \rightarrow \pi^0 n$:
    A68 V. D. Antopolsky et al. Phys. Lett. 28B, 223 (1968).
    D75 N. C. Debenham et al. Phys. Rev. 12D, 2545 (1975).
    K72 V. Kistiakowsky, et al. Phys. Rev. D6, 1882 (1972).
13. R. Kelly, (Particle Data Group, LBL), private communication.

TABLE CAPTION

I. Characteristics of charge -exchange scattering data[1] and maximum statistically significant order N_1.

II. Characteristics of polynomial representation of the B76 scattering data for $6 < N_1 < 14$.

III. Characteristics of charge-exchange polarization[2] and value of maximum statistically significant order N. The extrapolated values of the forward and backward differential cross section are plotted in Fig.3 for $N_1=10$; see the text for the evaluation of the errors on these quantities. The dispersion relation predictions are from Ref. [11].

IV. Zero locations of $\pi^- p$ charge-exchange data for $0.62 < p_{lab} < 2.7$ GeV/c , assuming all zeros to be outside the unit-circle in the w-plane, in different variables, z (= cosθ) , t and w . In the last column is the value of the outside boundary of the disc of convergence of the polynomial expansion, assuming the first singularity to be the rho meson.

V. Critical points and resolution of the discrete ambiguity.

FIGURE CAPTION

1. Chi-squared per data point vs. the polynomial order N_1 for the scattering data N72 (a) and B76 (b),detailed in (c).

2. Comparison of the polynomial representation of the B76 scattering data (N_1=10 , dotted line) with N72 data and polynomial representation thereof (N_1=6 (a) and N_1=10 (b,c,d) plain line) at 3 closely matched energies.(The data of B76 are in Figs. 12,19 and 23.)

3. (a) $(\frac{d\sigma}{d\Omega})_{\theta=0}$ from extrapolation of the 10th-order polynomial representation of B76 scattering data. The line is the value calculated in Ref.11.
   (b) $(\frac{d\sigma}{d\Omega})_{\theta=180}$ for extrapolation of the 10th-order polynomial representation of B76 scattering data, compared with the data of Ref. 12,(-□-)for D75, (-Δ-) for A69 and (-▽-) for K72.

4. Chi-squared per data point versus polynomial order N when B76 scattering and polarization data are simultanously analyzed. (a) for $\frac{d\sigma}{d\Omega}$. (b) for P.

5. Comparison of N=10 polynomial representation for P with S74 data at 3 closely-matched energies,(a) 1.030 (S74) and 1.027 (B76),(b) 1.440(S74) and 1.437 (B76) , (c) 1.590 (S74) and 1.601(B76).(The data of B76 are in Figs 12,17 and 19).

6 → 25. B76 data and N=10 polynomial representation thereof.

26. Location of the zeros of the 10th order polynomial fit in the w-plane for the 20 energies of the B76 data.

27. Re t versus $\sqrt{s}$ and p_{lab}, for trajectories of Σ^+ (-□-) and of Σ^- (-Δ-).

28 → 32. Detail of Fig. 27 with errors and corresponding location of the trajectories in the w-plane ,either ouside (with errors on the zero position) or inside the unit circle.

33. | w | versus p_{lab} , assuming all zeros outside,for the trajectories of (a) Σ^- (corresponding to maxima of the polarization), and (b) Σ^+ (corresponding to

minima of the polarization). Critical points are indicated according to their level of confidence increasing from one star (-□-), two stars (-■-), three stars (-O-) and four stars (-●-). The part of the trajectory which is found inside the unit-circle after the resolution of the discrete ambiguity, has been dotted. The curve above represents the outside boundary of the disc of convergence of the polynomial expansion, assuming the first singularity to be the rho.

TABLE I

	Plab (GeV/c)	Ref.	No. Pts.	cosθ interval (a)	N_1
1	0.618	B76	27	-.96/1.0	7
2	0.624	C67	20	-1.0/1.0	4
3	0.658	C67	20	-1.0/1.0	4
4	0.675	B76	30	-.96/1.0	13
5	0.718	C67	20	-1.0/1.0	4
6	0.724	B76	31	-.96/1.0	11
7	0.776	B76	31	-.96/1.0	11
8	0.782	C67	20	-1.0/1.0	5
9	0.825	B76	31	-.96/1.0	12
10	0.832	C67	20	-1.0/1.0	5
11	0.974	B76	34	-.96/1.0	13
12	1.004	C67	20	-1.0/1.0	5
13	1.027	B76	31	-.96/1.0	12
14	1.030	N72	87(88)	-.85/1.0[a]	13
15	1.060	B64	20	-1.0/1.0	2
16	1.077	B76	32	-.96/.94	9
17	1.105	C67	20	-1.0/1.0	7
18	1.170	B76	33	-.96/.96	11
19	1.248	C67	20	-1.0/1.0	7
20	1.275	B76	33	-.96/.96	13
21	1.356	B76	31	-.96/.94	9
22	1.432	C67	20	-1.0/1.0	7
23	1.438	B76	33	-.96/.96	13
24	1.505	B76	33	-.96/.96	11
25	1.590	N72	91(93)	-.85/1.0[a]	9
26	1.601	B76	33	-.96/.96	10
27	1.688	B76	34	-.96/.96	12
28	1.715	C69	40	-1.0/1.0	4
29	1.767	B76	34	-.96/.96	8
30	1.790	N72	87(88)	-.85/1.0[a]	7
31	1.872	B76	34	-.96/.96	13
32	1.889	C69	40	-1.0/1.0	7
33	1.975	B76	34	-.96/.96	10
34	1.990	N72	73(75)	-.85/1.0[a]	10
35	2.056	B76	34	-.96/.96	12
36	2.071	C69	40	-1.0/1.0	5
37	2.190	N72	70(72)	-.85/1.0[a]	5
38	2.265	C69	40	-1.0/1.0	11
39	2.267	B76	35	-.96/.96	12
40	2.390	N72	63(66)	-.85/1.0[a]	10
41	2.460	C69	40	-1.0/1.0	11

TABLE III

	Plab GeV/c)	Ref.	No. Pts.	cosθ interval	N
1	0.617	B76	17	-.70/.95	7
2	0.675	B76	20	-1.0/.95	13
3	0.723	B76	20	-1.0/.95	9
4	0.776	B76	20	-1.0/.95	11
5	0.827	B76	20	-1.0/.95	12
6	0.974	B76	20	-1.0/.95	13
7	1.027	B76	20	-1.0/.95	12
8	1.030	S74	20	-.92/.78	11
9	1.076	B76	20	-1.0/.95	13
10	1.170	B76	19	-1.0/.95	11
11	1.245	S74	19	-.84/.80	6
12	1.274	B76	20	-1.0/.95	13
13	1.355	B76	19	-1.0/.95	8
14	1.437	B76	20	-1.0/.95	9
15	1.440	S74	20	-.90/.81	9
16	1.505	B76	20	-1.0/.95	9
17	1.590	S74	20	-.90/.81	8
18	1.600	B76	20	-1.0/.95	8
19	1.687	B76	20	-1.0/.95	11
20	1.767	B76	20	-1.0/.95	8
21	1.790	S74	19	-.81/.82	8
22	1.871	B76	20	-1.0/.95	10
23	1.975	B76	19	-1.0/.95	10
24	2.055	B76	19	-1.0/.95	11
25	2.267	B76	17	-1.0/.95	12

(a) As explained in N72, data in the very backward direction ($-1 < \cos\theta < -.85$) where the chamber efficiency is low, have been omitted because of the systematic error in the correction which is large and thus the related data quite unreliable.

TABLE II

NO	PLAB	NPTS	N_1	χ^2/pt	$(\frac{d\sigma}{d\Omega})_{\theta=0^0}$ (mb/sr)			$(\frac{d\sigma}{d\Omega})_{\theta=180^0}$			[11] Disp. Rel.
1	.618	27	5	2.604	3.355			.0320			4.073
1	.618	27	6	2.254	3.474			.2752			4.073
1	.618	27	7	1.322	3.596			.0000			4.073
1	.618	27	8	1.068	3.627			.0673			4.073
1	.618	27	9	.889	3.573			.2736			4.073
1	.618	27	10	.876	3.546	.080	.100	.1410	.7800	.1400	4.073
1	.618	27	11	.867	3.539			.1801			4.073
1	.618	27	12	.764	3.564			.3675			4.073
1	.618	27	13	.672	3.508			.9153			4.073
1	.618	27	14	.621	3.448			.1617			4.073
2	.675	30	5	4.470	3.458			.3260			4.265
2	.675	30	6	4.769	3.491			.3938			4.265
2	.675	30	7	3.341	3.552			.2408			4.265
2	.675	30	8	3.402	3.544			.2160			4.265
2	.675	30	9	3.277	3.535			.2519			4.265
2	.675	30	10	3.325	3.543	.040	.010	.2926	.0001	.2910	4.265
2	.675	30	11	2.633	3.583			.0510			4.265
2	.675	30	12	2.669	3.575			.0001			4.265
2	.675	30	13	1.873	3.509			.6365			4.265
2	.675	30	14	1.814	3.544			1.0754			4.265
3	.724	31	5	4.568	2.573			.1879			3.248
3	.724	31	6	5.076	2.593			.2290			3.248
3	.724	31	7	2.918	2.700			.0001			3.248
3	.724	31	8	3.176	2.690			.0001			3.248
3	.724	31	9	1.689	2.631			.1608			3.248
3	.724	31	10	1.582	2.664	.120	.030	.3215	.0001	.3200	3.248
3	.724	31	11	.971	2.724			.0001			3.248
3	.724	31	12	1.001	2.722			.0001			3.248
3	.724	31	13	1.632	2.737			.0001			3.248
3	.724	31	14	.481	2.789			.4564			3.248
4	.776	31	5	3.624	1.542			.0001			1.986
4	.776	31	6	3.740	1.530			.0001			1.986
4	.776	31	7	6.710	1.588			.0001			1.986
4	.776	31	8	3.897	1.610			.0001			1.986
4	.776	31	9	3.821	1.610			.0001			1.986
4	.776	31	10	1.103	1.649	.040	.001	.0897	.1640	.0010	1.986
4	.776	31	11	2.830	1.681			.0001			1.986
4	.776	31	12	8.897	1.659			.0001			1.986
4	.776	31	13	4.512	1.646			.0001			1.986
4	.776	31	14	.543	1.679			.2539			1.986
5	.825	31	5	6.615	1.261			.0001			1.560
5	.825	31	6	8.705	1.172			.0001			1.560
5	.825	31	7	12.464	1.223			.0001			1.560
5	.825	31	8	6.884	1.268			.0001			1.560
5	.825	31	9	2.491	1.225			.0001			1.560
5	.825	31	10	.899	1.285	.010	.001	.2375	.0010	.0400	1.560
5	.825	31	11	.933	1.291			.2007			1.560
5	.825	31	12	3.466	1.239			.0001			1.560
5	.825	31	13	9.407	1.266			.0002			1.560
5	.825	31	14	12.312	1.255			.0002			1.560

NO	PLAB	NPTS	N_1	χ^2/pt	$(\frac{d\sigma}{d\Omega})_{\theta=0^0}$ (mb/sr)			$(\frac{d\sigma}{d\Omega})_{\theta=180^0}$			[11] Disp. Relations
11	1.356	31	6	4.686	.818			.3057			.051
11	1.356	31	7	1.696	.474			.5911			.051
11	1.356	31	8	1.616	.355			.4955			.051
11	1.356	31	9	1.321	.200			.6153			.051
11	1.356	31	10	1.310	.117	1.680	.103	.5532	.1200	.5530	.051
11	1.356	31	11	1.358	.238			.4656			.051
11	1.356	31	12	1.188	.014			.3091			.051
11	1.356	31	13	1.302	.617			.0002			.051
11	1.356	31	14	1.290	1.800			.6734			.051
12	1.438	33	6	8.459	.642			.2035			.120
12	1.438	33	7	2.505	.344			.5017			.120
12	1.438	33	8	2.351	.242			.4000			.120
12	1.438	33	9	1.723	.116			.5260			.120
12	1.438	33	10	1.705	.057	.640	.001	.4666	.0600	.4660	.120
12	1.438	33	11	1.661	.210			.3131			.120
12	1.438	33	12	1.570	.143			.2463			.120
12	1.438	33	13	2.002	.554			.0002			.120
12	1.438	33	14	1.111	.696			.0001			.120
13	1.505	33	6	7.809	.629			.1009			.267
13	1.505	33	7	2.034	.375			.3556			.267
13	1.505	33	8	1.957	.331			.3118			.267
13	1.505	33	9	1.846	.301			.3410			.267
13	1.505	33	10	1.848	.299	.480	.001	.3387	.0200	.3380	.267
13	1.505	33	11	1.694	.455			.1827			.267
13	1.505	33	12	1.660	.425			.1520			.267
13	1.505	33	13	1.863	.666			.0001			.267
13	1.505	33	14	1.423	.779			.0243			.267
14	1.601	33	6	5.365	.787			.0109			.467
14	1.601	33	7	1.510	.608			.1892			.467
14	1.601	33	8	1.367	.627			.2080			.467
14	1.601	33	9	1.119	.516			.3191			.467
14	1.601	33	10	.935	.369	.260	.080	.1726	.1400	.1720	.467
14	1.601	33	11	.935	.370			.1717			.467
14	1.601	33	12	.925	.346			.1474			.467
14	1.601	33	13	.906	.399			.0948			.467
14	1.601	33	14	.840	.295			.0001			.467
15	1.688	34	6	6.369	.723			.0000			.587
15	1.688	34	7	2.311	.593			.1180			.587
15	1.688	34	8	1.574	.666			.1912			.587
15	1.688	34	9	1.573	.668			.1891			.587
15	1.688	34	10	1.734	.584	.080	.270	.1052	.1000	.1050	.587
15	1.688	34	11	1.711	.489			.2008			.587
15	1.688	34	12	1.321	.318			.0299			.587
15	1.688	34	13	1.984	.443			.0001			.587
15	1.688	34	14	2.738	.393			.0001			.587

TABLE II (continued)

NO	PLAB	NPTS	N_1	χ^2/pt	$(\frac{d\sigma}{d\Omega})_{\theta=0^0}$ (mb/sr)			$(\frac{d\sigma}{d\Omega})_{\theta=180^0}$			[11] Disp. Rel.
6	.974	34	5	21.247	3.102			.0821			3.466
6	.974	34	6	19.521	2.884			.0002			3.466
6	.974	34	7	28.664	3.005			.0003			3.466
6	.974	34	8	27.002	3.017			.0003			3.466
6	.974	34	9	26.364	3.014			.0003			3.466
6	.974	34	10	3.903	3.109	.010	.010	.0001	.0100	.0100	3.466
6	.974	34	11	5.785	3.119			.0002			3.466
6	.974	34	12	20.685	3.071			.0003			3.466
6	.974	34	13	55.432	3.144			.0005			3.466
6	.974	34	14	64.685	3.129			.0006			3.466
7	1.027	31	5	6.827	2.432			.0661			2.887
7	1.027	31	6	6.942	2.036			.0002			2.887
7	1.027	31	7	7.065	1.817			.0002			2.887
7	1.027	31	8	8.189	1.473			.0002			2.887
7	1.027	31	9	2.508	.894			.0542			2.887
7	1.027	31	10	1.871	1.199	2.420	.310	.2285	.0010	.2280	2.887
7	1.027	31	11	2.022	1.554			.0391			2.887
7	1.027	31	12	5.612	.643			.0003			2.887
7	1.027	31	13	11.743	1.555			.0004			2.887
7	1.027	31	14	1.298	3.628			.0655			2.887
8	1.077	32	5	3.509	1.272			.0001			1.741
8	1.077	32	6	2.795	1.400			.0936			1.741
8	1.077	32	7	3.514	1.192			.2383			1.741
8	1.077	32	8	2.907	.989			.1062			1.741
8	1.077	32	9	1.416	.551			.3738			1.741
8	1.077	32	10	1.060	.808	1.450	.400	.5207	.0010	.5200	1.741
8	1.077	32	11	1.050	1.046			.3935			1.741
8	1.077	32	12	.763	.415			.0775			1.741
8	1.077	32	13	1.321	1.074			.0002			1.741
8	1.077	32	14	.496	2.258			.2887			1.741
9	1.171	33	5	13.123	.541			.0464			.525
9	1.171	33	6	4.916	.756			.2612			.525
9	1.171	33	7	2.794	.537			.4794			.525
9	1.171	33	8	2.417	.463			.4055			.525
9	1.171	33	9	2.071	.398			.4708			.525
9	1.171	33	10	1.893	.459	.350	.060	.5311	.0010	.5310	.525
9	1.171	33	11	1.942	.666			.3239			.525
9	1.171	33	12	1.828	.465			.1232			.525
9	1.171	33	13	1.692	.676			.0002			.525
9	1.171	33	14	1.491	.805			.0408			.525
10	1.275	33	6	4.517	.668			.3264			.148
10	1.275	33	7	2.000	.420			.5736			.148
10	1.275	33	8	1.474	.270			.4229			.148
10	1.275	33	9	1.200	.164			.5283			.148
10	1.275	33	10	1.187	.252	1.012	.090	.6162	.0010	.5290	.148
10	1.275	33	11	1.352	.421			.4475			.148
10	1.275	33	12	1.327	.537			.5634			.148
10	1.275	33	13	.850	1.013			.0872			.148
10	1.275	33	14	.883	1.264			.3378			.148

NO	PLAB	NPTS	N_1	χ^2/pt	$(\frac{d\sigma}{d\Omega})_{\theta=0^0}$ (mb/sr)			$(\frac{d\sigma}{d\Omega})_{\theta=180^0}$			[11] Disp. Relations
16	1.767	34	6	12.978	.673			.0000			.669
16	1.767	34	7	1.915	.555			.0508			.669
16	1.767	34	8	1.094	.645			.1412			.669
16	1.767	34	9	1.063	.673			.1138			.669
16	1.767	34	10	1.062	.643	.070	.090	.0840	.0600	.0830	.669
16	1.767	34	11	1.058	.636			.0904			.669
16	1.767	34	12	1.032	.594			.0482			.669
16	1.767	34	13	1.311	.710			.0000			.669
16	1.767	34	14	1.356	.705			.0000			.669
17	1.872	34	6	3.503	.633			.0037			.706
17	1.872	34	7	1.173	.548			.0886			.706
17	1.872	34	8	1.060	.582			.1229			.706
17	1.872	34	9	1.035	.626			.0786			.706
17	1.872	34	10	1.036	.632	.340	.080	.0841	.0400	.0840	.706
17	1.872	34	11	1.027	.653			.0631			.706
17	1.872	34	12	1.082	.690			.1005			.706
17	1.872	34	13	1.844	.886			.0000			.706
17	1.872	34	14	1.059	.968			.0000			.706
18	1.975	34	6	3.368	.549			.0288			.659
18	1.975	34	7	1.847	.488			.0893			.659
18	1.975	34	8	1.774	.541			.1419			.659
18	1.975	34	9	1.007	.608			.0753			.659
18	1.975	34	10	1.268	.484	.120	.290	.0000	.1420	.0010	.659
18	1.975	34	11	.604	.398			.0364			.659
18	1.975	34	12	.878	.322			.0000			.659
18	1.975	34	13	.527	.261			.0202			.659
18	1.975	34	14	.919	.192			.0000			.659
19	2.055	34	6	4.786	.542			.0800			.585
19	2.055	34	7	3.038	.479			.1425			.585
19	2.055	34	8	2.903	.538			.2017			.585
19	2.055	34	9	1.534	.618			.1222			.585
19	2.055	34	10	1.457	.480	.140	.390	.0000	.1220	.0010	.585
19	2.055	34	11	1.133	.291			.1730			.585
19	2.055	34	12	.754	.128			.0100			.585
19	2.055	34	13	.716	.086			.0521			.585
19	2.055	34	14	.693	.108			.0747			.585
20	2.267	35	6	3.093	.371			.1020			.304
20	2.267	35	7	2.024	.336			.1448			.304
20	2.267	35	8	2.037	.342			.1528			.304
20	2.267	35	9	1.565	363			.1256			.304
20	2.267	35	10	1.217	.275	.090	.180	.0045	.2500	.0010	.304
20	2.267	35	11	.791	.177			.1433			.304
20	2.267	35	12	.508	.108			.0404			.304
20	2.267	35	13	.472	.096			.0589			.304
20	2.267	35	14	.534	.215			.2489			.304

TABLE IV

TRAJ.	PLAB (GEV/C)	ECM (GEV)	Z		t (+) (GeV²)		W (++)		±δ(W) (++)		W_r (+++)	R_W (++
1A	.618	1.445	.273	-.060	-.234	-.019	.290	-1.024	.066	.126	1.064	5.502
1B	.618	1.445	.054	.327	-.305	.105	.070	1.378	.082	.103	1.379	5.502
1C	.618	1.445	-.682	-.214	-.541	-.069	-.868	-.998	.209	.226	1.323	5.502
1D	.618	1.445	1.098	.094	.032	.030	1.590	.305	.270	.112	1.619	5.502
1E	.618	1.445	-.990	-.031	-.641	-.010	-1.138	-.236	.166	.160	1.162	5.502
1F	.618	1.445	-.493	.162	-.481	.052	-.583	1.051	.089	.084	1.202	5.502
1G	.618	1.445	.817	-.232	-.059	-.075	1.095	-.913	.124	.105	1.425	5.502
1H	.618	1.445	.764	.343	-.076	.110	1.092	1.144	.151	.142	1.581	5.502
1I	.618	1.445	-.302	-.327	-.419	-.105	-.399	-1.340	.281	.225	1.398	5.502
1J	.618	1.445	-.859	.063	-.599	.020	-.962	.589	.075	.079	1.128	5.502
2A	.675	1.481	.386	-.194	-.225	-.071	.465	-1.140	.088	.088	1.231	5.044
2B	.675	1.481	.014	.349	-.361	.128	.018	1.409	.079	.122	1.409	5.044
2C	.675	1.481	-.602	-.139	-.586	-.051	-.705	-.956	.076	.084	1.188	5.044
2D	.675	1.481	1.138	.128	.051	.047	1.723	.378	.454	.236	1.764	5.044
2E	.675	1.481	-.976	-.024	-.723	-.009	-1.074	-.265	.285	.081	1.107	5.044
2F	.675	1.481	-.439	.137	-.526	.050	-.505	1.048	.052	.054	1.163	5.044
2G	.675	1.481	.916	-.324	-.031	-.118	1.354	-1.001	.376	.209	1.684	5.044
2H	.675	1.481	.767	.412	-.085	.151	1.139	1.261	.265	.162	1.700	5.044
2I	.675	1.481	-.127	-.277	-.412	-.101	-.161	-1.308	.143	.147	1.317	5.044
2J	.675	1.481	-.884	.181	-.689	.066	-1.163	.755	.209	.102	1.386	5.044
3A	.724	1.511	.206	-.160	-.321	-.065	.239	-1.152	.086	.086	1.176	4.722
3B	.724	1.511	-.011	.330	-.409	.133	-.014	1.382	.093	.099	1.382	4.722
3C	.724	1.511	-.396	-.135	-.564	-.055	-.454	-1.065	.051	.060	1.158	4.722
3D	.724	1.511	1.102	.019	.041	.008	1.567	.065	.195	.147	1.568	4.722
3E	.724	1.511	-1.028	-.029	-.819	-.012	-1.288	-.142	.282	.206	1.296	4.722
3F	.724	1.511	-.413	.148	-.571	.060	-.479	1.073	.060	.062	1.175	4.722
3G	.724	1.511	.688	-.298	-.126	-.121	.937	-1.122	.181	.141	1.462	4.722
3H	.724	1.511	.788	.320	-.086	.129	1.117	1.088	.111	.084	1.559	4.722
3I	.724	1.511	-.344	-1.351	-.543	-.546	-.623	-3.019	2.568	3.052	3.083	4.722
3J	.724	1.511	-.912	.070	-.773	.028	-1.057	.510	.128	.166	1.173	4.722
4A	.776	1.543	.493	-.192	-.248	-.085	.535	-1.113	.067	.073	1.235	4.436
4B	.776	1.543	-.041	.279	-.464	.124	-.052	1.316	.085	.061	1.317	4.436
4C	.776	1.543	-.189	-.153	-.530	-.068	-.218	-1.148	.064	.044	1.168	4.436
4D	.776	1.543	1.077	.101	.034	.045	1.531	.341	.190	.125	1.568	4.436
4E	.776	1.543	-1.006	-.004	-.894	-.002	-1.121	-.044	.216	.127	1.122	4.436
4F	.776	1.543	-.487	.257	-.662	.115	-.623	1.178	.184	.156	1.333	4.436
4G	.776	1.543	.859	-.215	-.063	-.096	1.152	-.844	.122	.107	1.428	4.436
4H	.776	1.543	.728	.294	-.121	.131	.997	1.088	.077	.072	1.476	4.436
4I	.776	1.543	-.564	-.640	-.697	-.285	-.893	-1.735	.345	.653	1.951	4.436
4J	.776	1.543	-.933	.079	-.861	.035	-1.112	.489	.202	.157	1.214	4.436
5A	.825	1.572	.619	-.088	-.185	-.043	.688	-.881	.039	.048	1.118	4.206
5B	.825	1.572	-.126	.246	-.547	.119	-.157	1.269	.052	.067	1.278	4.206
5C	.825	1.572	-.297	-.137	-.629	-.067	-.339	-1.103	.042	.060	1.154	4.206
5D	.825	1.572	.525	.375	-.230	.182	.732	1.328	.142	.117	1.516	4.206
5E	.825	1.572	-1.004	-.029	-.972	-.014	-1.188	-.189	.090	.089	1.202	4.206
5F	.825	1.572	-.610	.638	-.781	.310	-.970	1.717	.522	.500	1.972	4.206
5G	.825	1.572	.967	-.147	-.016	-.071	1.292	-.584	.082	.117	1.418	4.206
5H	.825	1.572	.902	.209	-.047	.101	1.228	.788	.104	.076	1.459	4.206
5I	.825	1.572	.039	-.225	-.466	-.109	.047	-1.249	.088	.074	1.250	4.206
5J	.825	1.572	-.933	.061	-.938	.029	-1.077	.453	.070	.082	1.168	4.206

TRAJ.	PLAB (GEV/C)	ECM (GEV)	Z		t (+) (GeV²)		W (++)		±δ(W) (++)		W_r (+++)	R_W (+++)
11A	1.356	1.860	.626	-.127	-.350	-.119	.726	-.923	.030	.026	1.175	2.925
11B	1.356	1.860	.060	.243	-.880	.228	.074	1.271	.084	.097	1.273	2.925
11C	1.356	1.860	-.209	-.110	-1.132	-.103	-.232	-1.094	.024	.028	1.119	2.925
11D	1.356	1.860	.278	.687	-.676	.643	.438	1.878	.750	.849	1.929	2.925
11E	1.356	1.860	-.914	-.023	-1.792	-.021	-.965	-.432	.040	.028	1.057	2.925
11F	1.356	1.860	-.672	.103	-1.565	.097	-.764	.857	.035	.032	1.148	2.925
11G	1.356	1.860	.999	.013	-.001	.012	1.110	.130	.340	.169	1.118	2.925
11H	1.356	1.860	.835	.228	-.154	.213	1.123	.889	.209	.271	1.432	2.925
11I	1.356	1.860	.069	-.684	-.872	-.640	.107	-1.894	.323	.332	1.897	2.925
11J	1.356	1.860	-1.197	.105	-2.056	.098	-1.871	.290	.384	.327	1.894	2.925
12A	1.438	1.900	.605	-.123	-.398	-.124	.697	-.933	.022	.022	1.165	2.822
12B	1.438	1.900	.139	.136	-.869	.137	.157	1.136	.028	.047	1.147	2.822
12C	1.438	1.900	-.276	-.080	-1.286	-.080	-.299	-1.045	.014	.020	1.086	2.822
12D	1.438	1.900	.308	1.333	-.698	1.344	.555	2.989	1.741	1.613	3.040	2.822
12E	1.438	1.900	-.910	-.028	-1.926	-.028	-.971	-.448	.028	.020	1.070	2.822
12F	1.438	1.900	-.666	.121	-1.679	.122	-.771	.884	.024	.024	1.173	2.822
12G	1.438	1.900	1.040	-.012	.040	-.012	1.327	-.056	.122	.066	1.328	2.822
12H	1.438	1.900	.719	.182	-.284	.183	.895	.922	.055	.055	1.285	2.822
12I	1.438	1.900	.385	-.912	-.620	-.920	.650	-2.237	.505	.600	2.330	2.822
12J	1.438	1.900	-1.154	.112	-2.172	.113	-1.760	.326	.248	.266	1.789	2.822
13A	1.505	1.933	.574	-.130	-.455	-.138	.664	-.963	.026	.022	1.170	2.747
13B	1.505	1.933	.186	.153	-.869	.163	.214	1.148	.037	.051	1.168	2.747
13C	1.505	1.933	-.282	-.058	-1.368	-.062	-.299	-1.020	.014	.028	1.063	2.747
13D	1.505	1.933	-2.062	.031	-3.268	.033	-3.865	.066	5.410	5.789	3.865	2.747
13E	1.505	1.933	-.910	-.058	-2.039	-.062	-1.031	-.493	.035	.024	1.143	2.747
13F	1.505	1.933	-.677	.161	-1.790	.172	-.819	.928	.039	.046	1.238	2.747
13G	1.505	1.933	1.057	-.034	.060	-.037	1.411	-.137	.210	.165	1.418	2.747
13H	1.505	1.933	.642	.138	-.383	.147	.754	.925	.036	.048	1.193	2.747
13I	1.505	1.933	1.326	-.457	.348	-.488	2.297	-1.082	1.297	1.661	2.539	2.747
13J	1.505	1.933	-1.144	.229	-2.289	.244	-1.792	.633	.734	.804	1.900	2.747
14A	1.601	1.979	.592	-.157	-.471	-.181	.703	-.986	.042	.042	1.211	2.652
14B	1.601	1.979	.278	.117	-.832	.135	.312	1.086	.042	.060	1.130	2.652
14C	1.601	1.979	-.324	-.047	-1.526	-.054	-.340	-.994	.014	.032	1.050	2.652
14D	1.601	1.979	-.515	.600	-1.747	.691	-.800	1.684	.419	.420	1.864	2.652
14E	1.601	1.979	-.919	-.046	-2.212	-.053	-1.023	-.457	.045	.035	1.120	2.652
14F	1.601	1.979	-.746	.148	-2.012	.171	-.904	.849	.062	.057	1.240	2.652
14G	1.601	1.979	1.002	-.073	.002	-.084	1.271	-.346	.096	.089	1.317	2.652
14H	1.601	1.979	.654	.100	-.399	.116	.739	.869	.040	.047	1.141	2.652
14I	1.601	1.979	.751	-.800	-.287	-.922	1.269	-1.959	.745	.756	2.334	2.652
14J	1.601	1.979	-1.146	.008	-2.473	.009	-1.705	.023	.466	.381	1.706	2.652
15A	1.688	2.020	.562	-.144	-.539	-.178	.658	-.990	.033	.030	1.188	2.576
15B	1.688	2.020	.330	.218	-.824	.268	.404	1.189	.087	.084	1.256	2.576
15C	1.688	2.020	-.333	-.000	-1.640	-.000	-.333	-.993	0.000	0.000	1.000	2.576
15D	1.688	2.020	-.347	.527	-1.657	.649	-.515	1.616	.228	.279	1.696	2.576
15E	1.688	2.020	-.901	-.043	-2.339	-.053	-.989	-.487	.041	.036	1.102	2.576
15F	1.688	2.020	-.785	.137	-2.196	.169	-.950	.793	.056	.054	1.237	2.576
15G	1.688	2.020	.944	-.064	-.068	-.079	1.107	-.437	.062	.047	1.190	2.576
15H	1.688	2.020	.637	.079	-.446	.097	.702	.856	.041	.052	1.107	2.576
15I	1.688	2.020	.887	-1.248	-.138	-1.535	1.617	-2.765	1.255	1.657	3.204	2.576
15J	1.688	2.020	-1.100	.024	-2.583	.029	-1.559	.080	.381	.299	1.561	2.576

TABLE IV (continued)

TRAJ.	PLAB (GEV/C)	ECM (GEV)	Z		t (+) (GeV²)		W (++)		±δ(W) (++)		W_r (+++)	R_W (++
6A	.974	1.657	.642	-.054	-.218	-.033	.687	-.824	.017	.017	1.073	3.678
6B	.974	1.657	.019	.095	-.597	.058	.021	1.099	.047	.065	1.099	3.678
6C	.974	1.657	-.275	.000	-.776	.000	-.275	-.961	0.000	0.000	1.000	3.678
6D	.974	1.657	.869	.376	-.080	.229	1.301	1.133	.395	.274	1.725	3.678
6E	.974	1.657	-1.134	-.026	-1.298	-.016	-1.672	-.080	.243	.168	1.674	3.678
6F	.974	1.657	-.313	.361	-.799	.219	-.424	1.383	.096	.117	1.446	3.678
6G	.974	1.657	1.020	-.213	.012	-.130	1.485	-.682	.106	.146	1.634	3.678
6H	.974	1.657	.604	.276	-.241	.168	.796	1.141	.128	.156	1.391	3.678
6I	.974	1.657	-.239	-.610	-.754	-.371	-.366	-1.763	.165	.152	1.801	3.678
6J	.974	1.657	-1.000	.000	-1.216	.000	-1.000	-.019	0.000	0.000	1.000	3.678
7A	1.027	1.687	.651	-.029	-.228	-.019	.676	-.790	.028	.028	1.039	3.534
7B	1.027	1.687	.045	.000	-.623	.000	.045	.999	0.000	0.000	1.000	3.534
7C	1.027	1.687	-.257	.000	-.820	.000	-.257	-.966	0.000	0.000	1.000	3.534
7D	1.027	1.687	1.542	.574	.354	.375	2.787	1.284	2.260	2.185	3.069	3.534
7E	1.027	1.687	-1.004	-.018	-1.308	-.011	-1.152	-.137	.133	.126	1.160	3.534
7F	1.027	1.687	-.288	.289	-.841	.189	-.371	1.293	.078	.085	1.345	3.534
7G	1.027	1.687	1.113	-.033	.074	-.022	1.608	-.107	.356	.267	1.611	3.534
7H	1.027	1.687	.716	.229	-.185	.150	.931	.994	.093	.082	1.362	3.534
7I	1.027	1.687	-.400	-.625	-.914	-.408	-.622	-1.756	.218	.202	1.863	3.534
7J	1.027	1.687	-1.089	.066	-1.364	.043	-1.544	.224	.284	.211	1.560	3.534
8A	1.077	1.714	.667	.000	-.232	.000	.667	-.745	0.000	0.000	1.000	3.413
8B	1.077	1.714	.014	.068	-.685	.047	.015	1.070	.033	.067	1.070	3.413
8C	1.077	1.714	-.215	-.075	-.844	-.052	-.231	-1.055	.014	.024	1.080	3.413
8D	1.077	1.714	1.379	.332	.263	.231	2.380	.791	1.285	1.074	2.507	3.413
8E	1.077	1.714	-.967	-.036	-1.368	-.025	-1.090	-.320	.024	.045	1.136	3.413
8F	1.077	1.714	-.335	.161	-.928	.112	-.392	1.119	.041	.039	1.186	3.413
8G	1.077	1.714	1.128	-.113	.089	-.079	1.687	-.342	.264	.442	1.722	3.413
8H	1.077	1.714	.793	.130	-.144	.090	.953	.773	.037	.037	1.227	3.413
8I	1.077	1.714	-.567	-.538	-1.089	-.374	-.864	-1.565	.177	.157	1.787	3.413
8J	1.077	1.714	-.991	.153	-1.384	.106	-1.354	.571	.101	.067	1.469	3.413
9A	1.171	1.764	.671	-.103	-.255	-.080	.763	-.857	.022	.022	1.147	3.218
9B	1.171	1.764	-.098	.281	-.851	.218	-.124	1.315	.100	.111	1.321	3.218
9C	1.171	1.764	-.150	-.070	-.892	-.054	-.161	-1.061	.010	.017	1.073	3.218
9D	1.171	1.764	.974	.699	-.020	.542	1.655	1.700	1.036	1.014	2.372	3.218
9E	1.171	1.764	-.935	-.030	-1.500	-.023	-1.012	-.396	.030	.026	1.086	3.218
9F	1.171	1.764	-.439	.142	-1.116	.110	-.507	1.054	.081	.074	1.169	3.218
9G	1.171	1.764	1.091	-.126	.071	-.098	1.591	-.402	.220	.285	1.641	3.218
9H	1.171	1.764	.846	.123	-.119	.096	1.027	.700	.057	.057	1.243	3.218
9I	1.171	1.764	-.651	-.729	-1.280	-.565	-1.070	-1.862	.335	.355	2.147	3.218
9J	1.171	1.764	-.972	.281	-1.529	.218	-1.435	.872	.234	.190	1.679	3.218
10A	1.275	1.818	.627	-.096	-.323	-.083	.703	-.884	.022	.017	1.130	3.041
10B	1.275	1.818	-.107	.206	-.958	.178	-.128	1.222	.060	.066	1.229	3.041
10C	1.275	1.818	-.104	-.101	-.955	-.087	-.114	-1.101	.022	.030	1.107	3.041
10D	1.275	1.818	.306	.397	-.600	.344	.424	1.435	.136	.157	1.497	3.041
10E	1.275	1.818	-.916	-.000	-1.658	-.000	-.916	-.401	0.000	0.000	1.000	3.041
10F	1.275	1.818	-.633	.066	-1.414	.057	-.687	.844	.047	.047	1.088	3.041
10G	1.275	1.818	1.003	-.006	.003	-.005	1.101	-.067	.227	.075	1.103	3.041
10H	1.275	1.818	.846	.044	-.133	.038	.915	.583	.082	.057	1.085	3.041
10I	1.275	1.818	-.333	-.471	-1.153	-.408	-.480	-1.536	.138	.142	1.609	3.041
10J	1.275	1.818	-1.132	.138	-1.846	.120	-1.712	.409	.236	.225	1.760	3.041
16A	1.767	2.056	.580	-.118	-.547	-.154	.663	-.946	.026	.030	1.155	2.514
16B	1.767	2.056	.332	.255	-.869	.332	.418	1.237	.097	.104	1.305	2.514
16C	1.767	2.056	-.341	-.051	-1.744	-.066	-.359	-.992	.014	.028	1.055	2.514
16D	1.767	2.056	-.457	.405	-1.896	.527	-.643	1.400	.200	.178	1.540	2.514
16E	1.767	2.056	-.917	-.055	-2.493	-.071	-1.036	-.476	.066	.048	1.140	2.514
16F	1.767	2.056	-.855	.141	-2.412	.183	-1.063	.718	.107	.114	1.283	2.514
16G	1.767	2.056	.957	-.062	-.056	-.081	1.129	-.407	.071	.060	1.200	2.514
16H	1.767	2.056	.627	.080	-.486	.104	.691	.866	.044	.046	1.108	2.514
16I	1.767	2.056	1.232	-1.295	.302	-1.684	2.290	-2.803	2.152	2.228	3.620	2.514
16J	1.767	2.056	-1.136	.012	-2.778	.016	-1.674	.037	.750	.507	1.674	2.514
17A	1.872	2.103	.557	-.118	-.618	-.164	.635	-.960	.032	.028	1.151	2.440
17B	1.872	2.103	.167	.169	-1.163	.236	.195	1.170	.040	.045	1.186	2.440
17C	1.872	2.103	-.330	-.070	-1.856	-.098	-.355	-1.017	.017	.026	1.077	2.440
17D	1.872	2.103	-.525	.249	-2.127	.347	-.670	1.147	.062	.069	1.328	2.440
17E	1.872	2.103	-.807	-.166	-2.521	-.232	-1.013	-.814	.083	.062	1.300	2.440
17F	1.872	2.103	-.841	.105	-2.568	.146	-.995	.677	.044	.054	1.203	2.440
17G	1.872	2.103	.471	-.076	-.041	-.107	1.192	-.412	.131	.145	1.261	2.440
17H	1.872	2.103	.645	.034	-.496	.047	.673	.800	.039	.039	1.045	2.440
17I	1.872	2.103	1.207	-.198	.288	-.277	1.931	-.529	.696	.600	2.002	2.440
17J	1.872	2.103	-.988	-.022	-2.774	-.030	-1.100	-.213	.147	.118	1.120	2.440
18A	1.975	2.148	.518	-.181	-.718	-.269	.624	-1.062	.051	.049	1.232	2.376
18B	1.975	2.148	.250	.363	-1.117	.540	.337	1.401	.194	.179	1.441	2.376
18C	1.975	2.148	-.339	-.023	-1.993	-.035	-.348	-.964	.024	.055	1.025	2.376
18D	1.975	2.148	-.283	.387	-1.909	.576	-.388	1.427	.176	.163	1.478	2.376
18E	1.975	2.148	-.804	-.091	-2.685	-.135	-.924	-.704	.032	.028	1.161	2.376
18F	1.975	2.148	-.747	.120	-2.599	.178	-.877	.808	.044	.039	1.192	2.376
18G	1.975	2.148	.856	-.158	-.214	-.235	1.086	-.745	.088	.117	1.317	2.376
18H	1.975	2.148	.656	.115	-.512	.171	.753	.885	.050	.050	1.162	2.376
18I	1.975	2.148	1.258	-.049	.383	-.073	2.023	-.130	.655	.478	2.027	2.376
18J	1.975	2.148	-1.000	-.000	-2.976	-.000	-1.000	.024	0.000	0.000	1.000	2.376
19A	2.055	2.183	.523	-.082	-.744	-.128	.573	-.940	.032	.042	1.101	2.331
19B	2.055	2.183	.159	.284	-1.312	.443	.204	1.312	.133	.132	1.328	2.331
19C	2.055	2.183	-.319	-.000	-2.058	-.000	-.319	-.948	0.000	0.000	1.000	2.331
19D	2.055	2.183	-.293	.416	-2.018	.650	-.410	1.466	.314	.214	1.522	2.331
19E	2.055	2.183	-.785	-.039	-2.786	-.061	-.835	-.661	.042	.047	1.065	2.331
19F	2.055	2.183	-.741	.087	-2.717	.136	-.835	.771	.047	.045	1.136	2.331
19G	2.055	2.183	.878	-.091	-.190	-.141	1.034	-.601	.057	.056	1.196	2.331
19H	2.055	2.183	.719	.097	-.438	.151	.818	.805	.037	.042	1.148	2.331
19I	2.055	2.183	1.973	.077	1.518	.120	3.674	.166	2.369	2.030	3.678	2.331
19J	2.055	2.183	-1.010	.001	-3.137	.002	-1.155	.011	.157	.079	1.155	2.331
20A	2.267	2.260	.504	-.171	-.879	-.303	.602	-1.057	.109	.141	1.216	2.218
20B	2.267	2.260	-.008	.246	-1.786	.436	-.010	1.276	.162	.165	1.276	2.218
20C	2.267	2.260	-.301	-.074	-2.306	-.132	-.325	-1.031	.026	.026	1.081	2.218
20D	2.267	2.260	-.276	.436	-2.261	.773	-.389	1.498	.489	.365	1.547	2.218
20E	2.267	2.260	-.772	-.100	-3.140	-.177	-.890	-.754	.044	.044	1.166	2.218
20F	2.267	2.260	-.742	.000	-3.087	.000	-.742	.670	0.000	0.000	1.000	2.218
20G	2.267	2.260	.733	-.038	-.474	-.068	.774	-.721	.094	.118	1.058	2.218
20H	2.267	2.260	.707	.208	-.520	.368	.899	.970	.121	.081	1.322	2.218
20I	2.267	2.260	1.053	.092	.094	.162	1.452	.334	.170	.151	1.490	2.218
20J	2.267	2.260	-1.006	-.005	-3.554	-.010	-1.122	-.053	.153	.076	1.123	2.218

(+) SEE FIG.(27) FOR PLOTS OF (RET VS ECM).
(++) SEE FIGS. (26) FOR PLOTS IN W-PLANE.
(ERRORS ON THE CRITICAL POINT POSITIONS HAVE BEEN ARTIFICIALLY SET TO ZERO FOR COMMODITY. SEE REF. (10) FOR DETAILS.)
(+++) SEE FIG.(33) FOR THE PLOT OF THE DISTANCE TO THE PHYSICAL REGION IN THE W-PLANE VS PLAB.
(THESE DISTANCES HAVE BEEN CALCULATED BEFORE THE RESOLUTION OF THE DISCRETE AMBIGUITY, ASSUMING ALL TRAJECTORIES IN THE W-PLANE ARE OUTSIDE THE UNIT CIRCLE.
SOLUTIONS INSIDE WOULD HAVE - IM(Z) AND IM(T) CHANGED SIGN,
- W REPLACED BY CONJ(1./W),
- WR AND RW REPLACED BY THEIR INVERSE.)

TABLE V

P_{lab} (GeV/c)	Critical points† 4*	3*	2*	1*	Discrete ambiguity A	B	C	D	E	F	G	H	I	J.
					I	I	I	I	I	0	0	0	0	0
0.618		A												
					0	I	I	I	I	0	0	0	0	0
0.675														
					0	I	I	I	I	0	0	0	0	0
0.724														
					0	I	I	I	I	0	0	0	0	0
0.776		J												
					0	I	I	I	I	0	0	0	0	0/I
0.825		J												
					0	I	I	I	I	0	0	0	0	0/I
0.974	C	B,C,J	J											
					0	I/0	I/0	I	I	0	0	0	0	I
1.027	B	A,B,C	C											
					0/I	I/0	0/I	I	I	0	0	0	0	I
1.077		A,B	A											
					I	0	I	I	I	0	0	0	0	I
1.170		E												
					I	0	I	I	I/0	0	0	0	0	I
1.275	E	E,F,H												
				F,H	I	0	I	I	0	0/I	0	0/I	0	I

P_{lab} (GeV/c)	Critical points† 4*	3*	2*	1*	Discrete ambiguity†† A	B	C	D	E	F	G	H	I	J
					I	0	I	I	0	0/I	0	0/I	0	I
1.356		G												
					I	0	I	I	0	I	I	I	0	I
1.438		E												
				B	I	0/I	I	I	I	I	I	I	0	I
1.505														
					I	I	I	I	I	I	I	I	0	I
1.601		C												
					I	I	I/0	I	I	I	I	I	0	I
1.688	C	C,E												
				B,E	I	I/0	I/0	I	I/0	I	I	I	0	I
1.767		C												
					I	0	0	I	0	I	I	I	0	I
1.872		G,H												
			A,G,H		I/0	0	0	I	0	I	0	I/0	0	I
1.975		C,J	J											
					0	0	0/I	I	0	I	0	0	0	0
2.055		C	C											
				A,E	0/I	0	I	I	0/I	0	0	0	0	0
2.267		F,J	F											
					I	0	I	I	I	0	0	0	0	I

† 4* : Data and polynomial approximation show that $|P| = 1$.
3* : Data have been renormalized (by 10%) for data and polynomial approximation to show $|P|=1$.
2* : Data are missing at the $\cos\theta$ value where the polynomial approximation shows that $|P|=1$.
1* : Data are missing at the p_{lab} value (within 2 of the B76 p_{lab} values) where we beleive a critical point would be observed.

††The trajectories are named after their location at $p_{lab} = 1.438$ GeV/c (see Fig. 26) and are found either inside (I) or outside (0) of the unit circle in the w-plane.

0 0 0 0 4 8 0 2 6 3 7

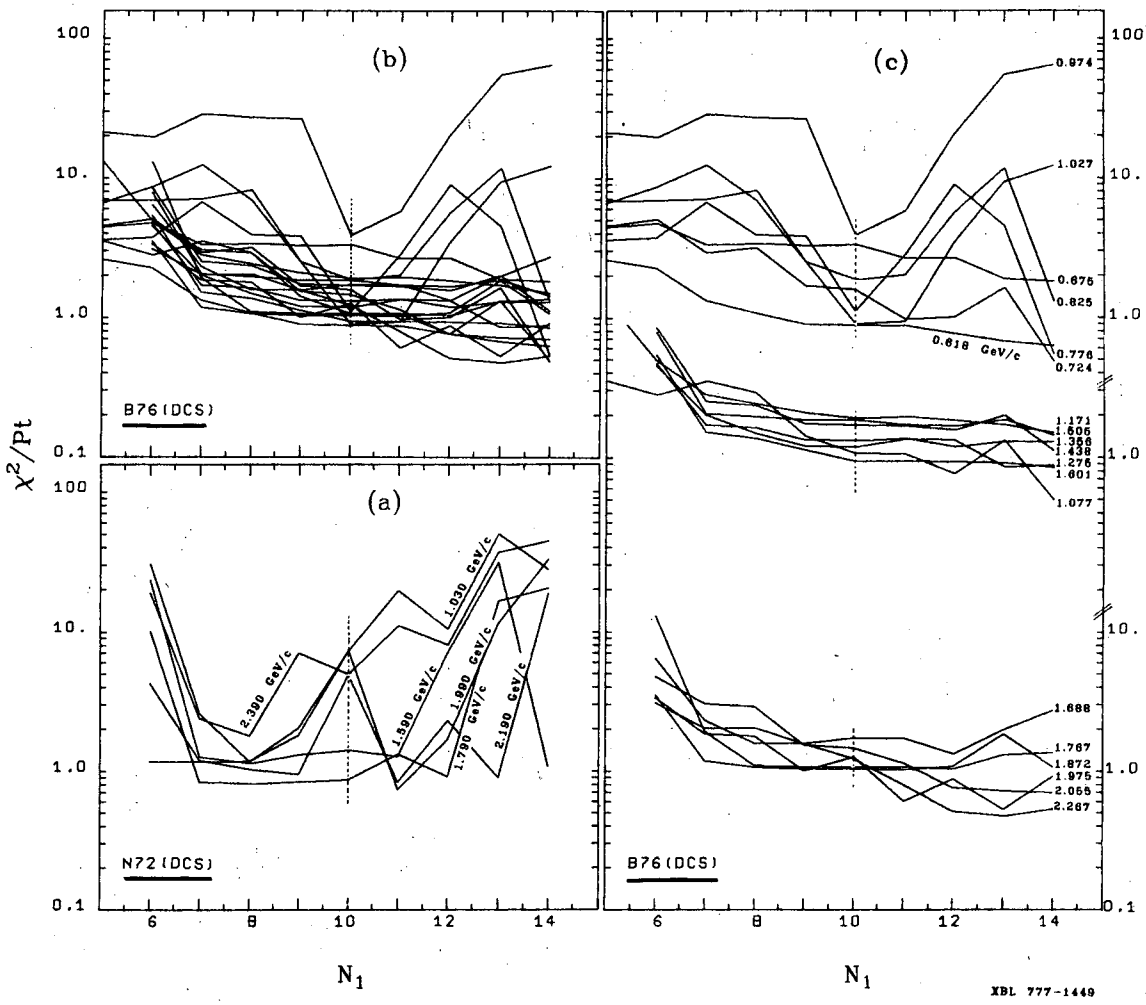

Figure 1

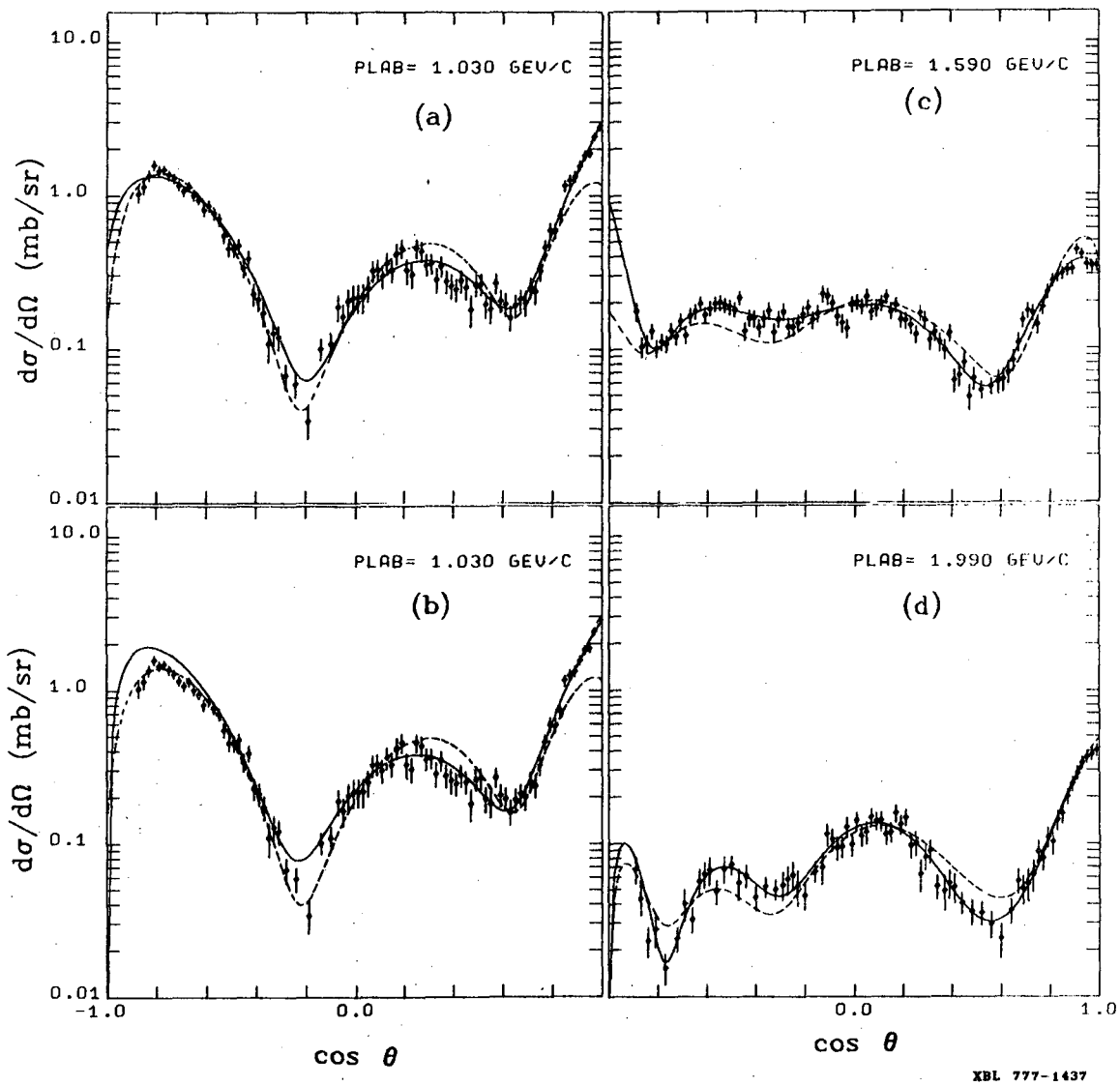
PLAB= 1.030 GEV/C
(a)
PLAB= 1.590 GEV/C
(c)
PLAB= 1.030 GEV/C
(b)
PLAB= 1.990 GEV/C
(d)
10.0
1.0
0.1
0.01
dσ/dΩ (mb/sr)
-1.0
0.0
1.0
cos θ
XBL 777-1437

Figure 2

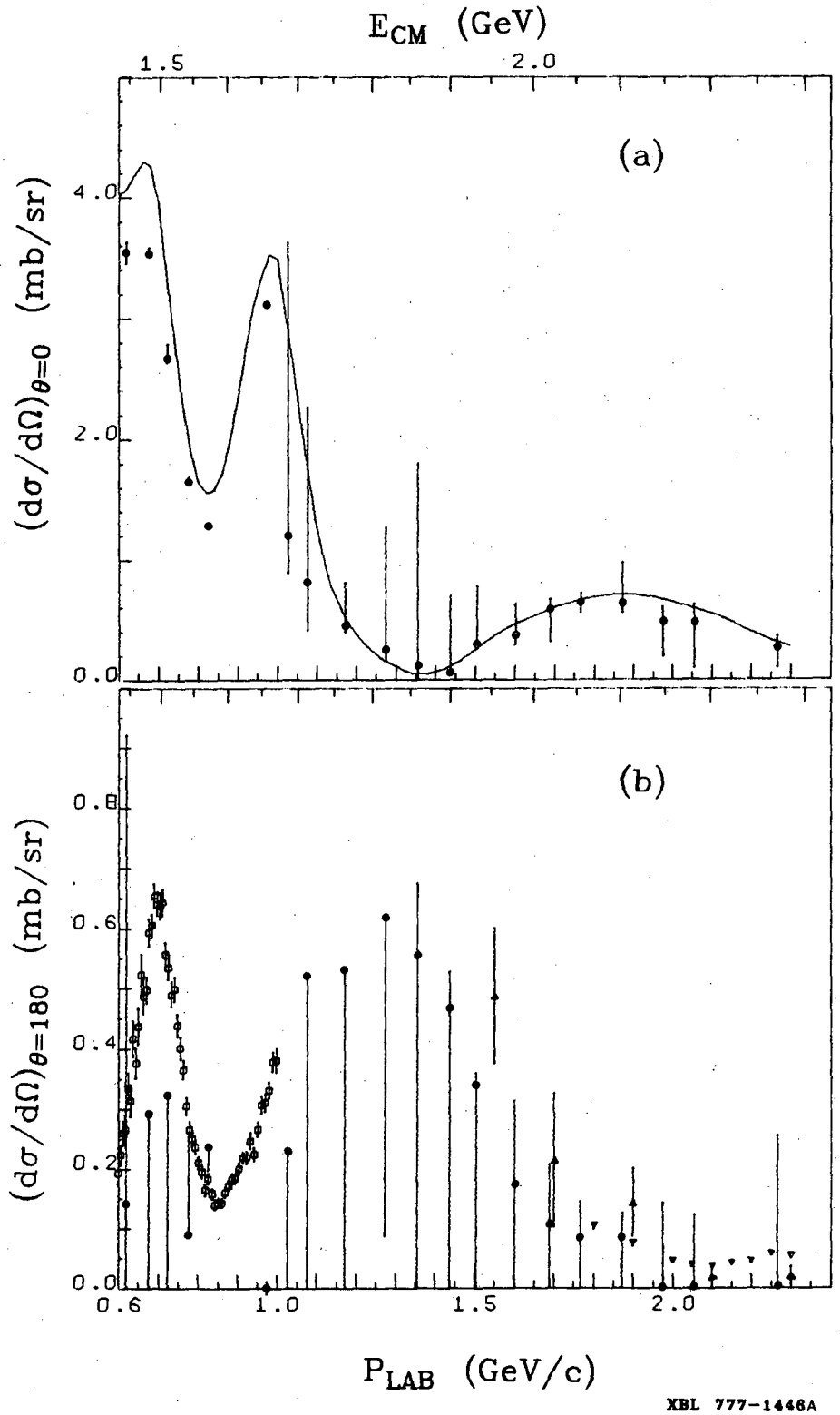
E_CM (GeV)
1.5
2.0
(a)
4.0
2.0
0.0
(dσ/dΩ)θ=0 (mb/sr)
(b)
0.8
0.6
0.4
0.2
0.0
(dσ/dΩ)θ=180 (mb/sr)
0.6
1.0
1.5
2.0
P_LAB (GeV/c)
XBL 777-1446A

Figure 3

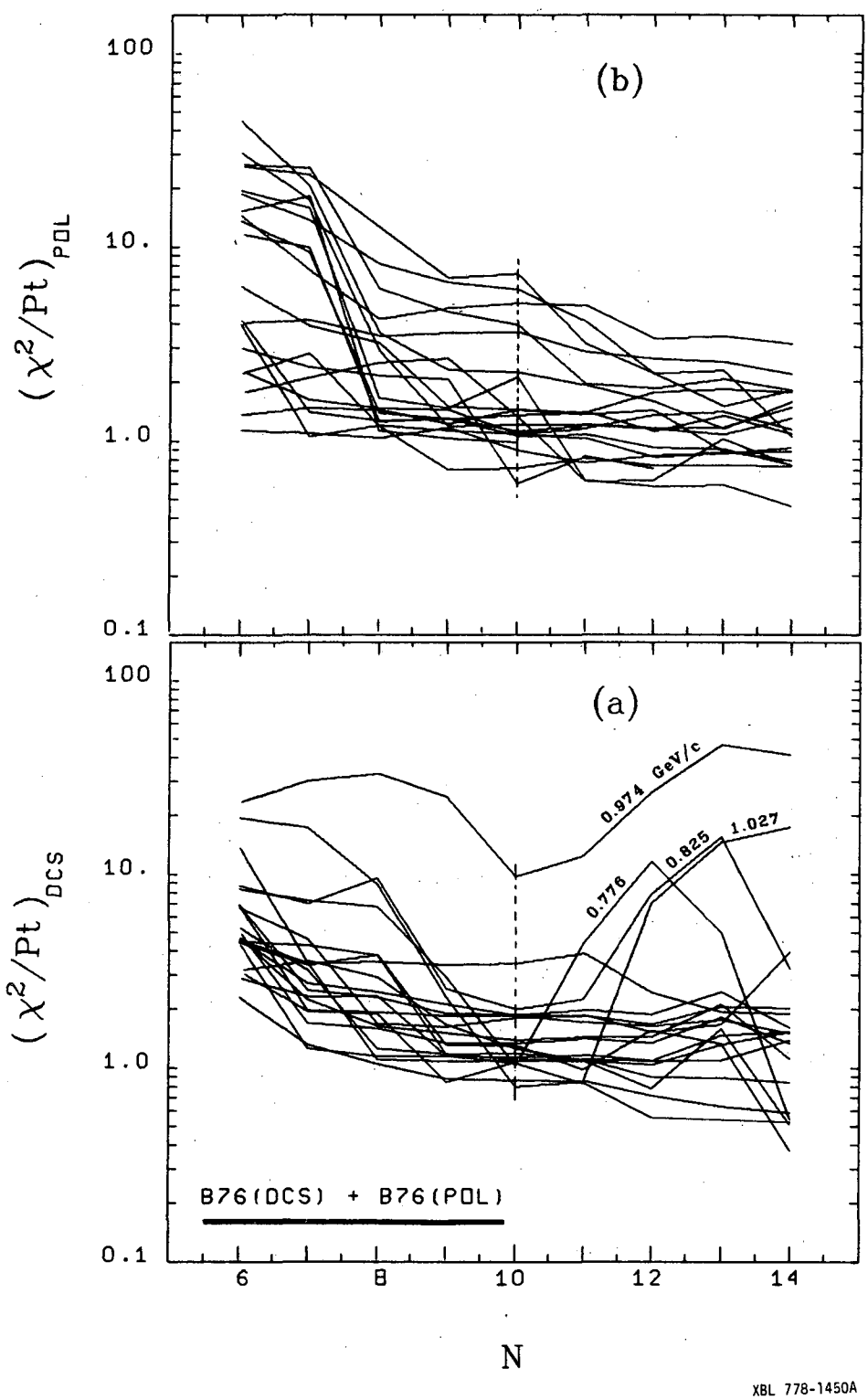
(b)
(a)
$(\chi^2/Pt)_{POL}$
$(\chi^2/Pt)_{DCS}$
100
10.
1.0
0.1
0.974 GeV/c
0.776
0.825
1.027
B76(DCS) + B76(POL)
6
8
10
12
14
N
XBL 778-1450A

Figure 4

0 0 0 0 4 8 0 2 6 3 8

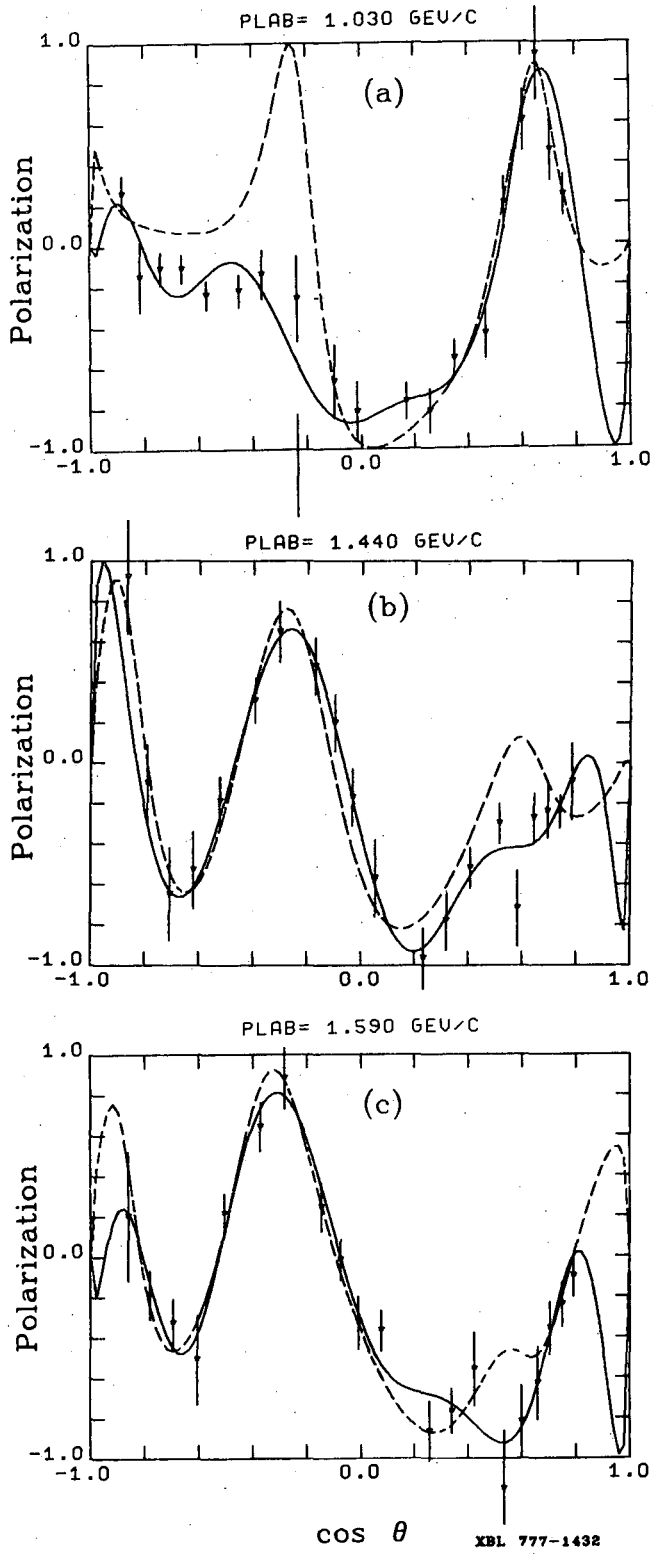

Figure 5

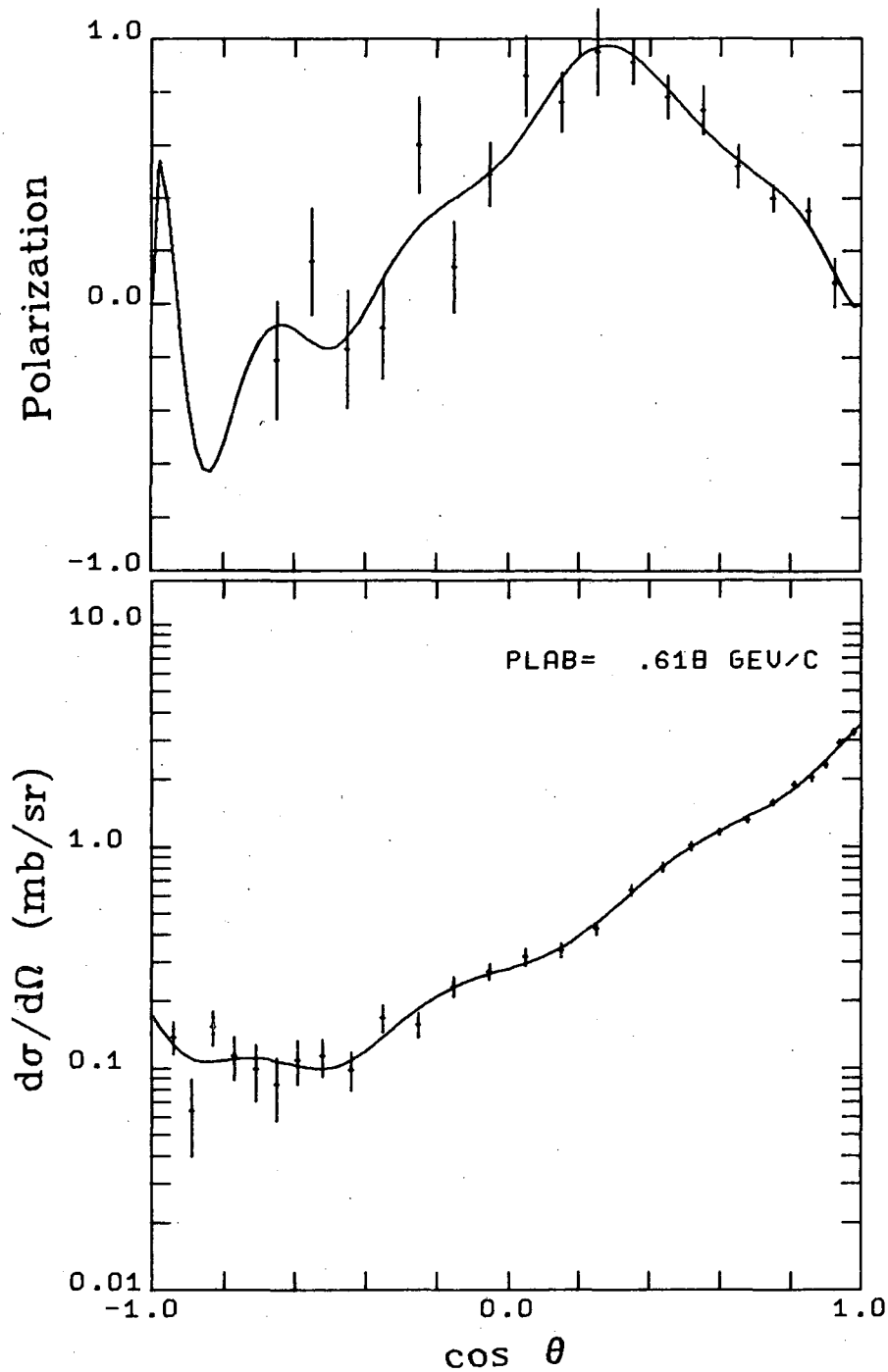

XBL 776-1268

Figure 6

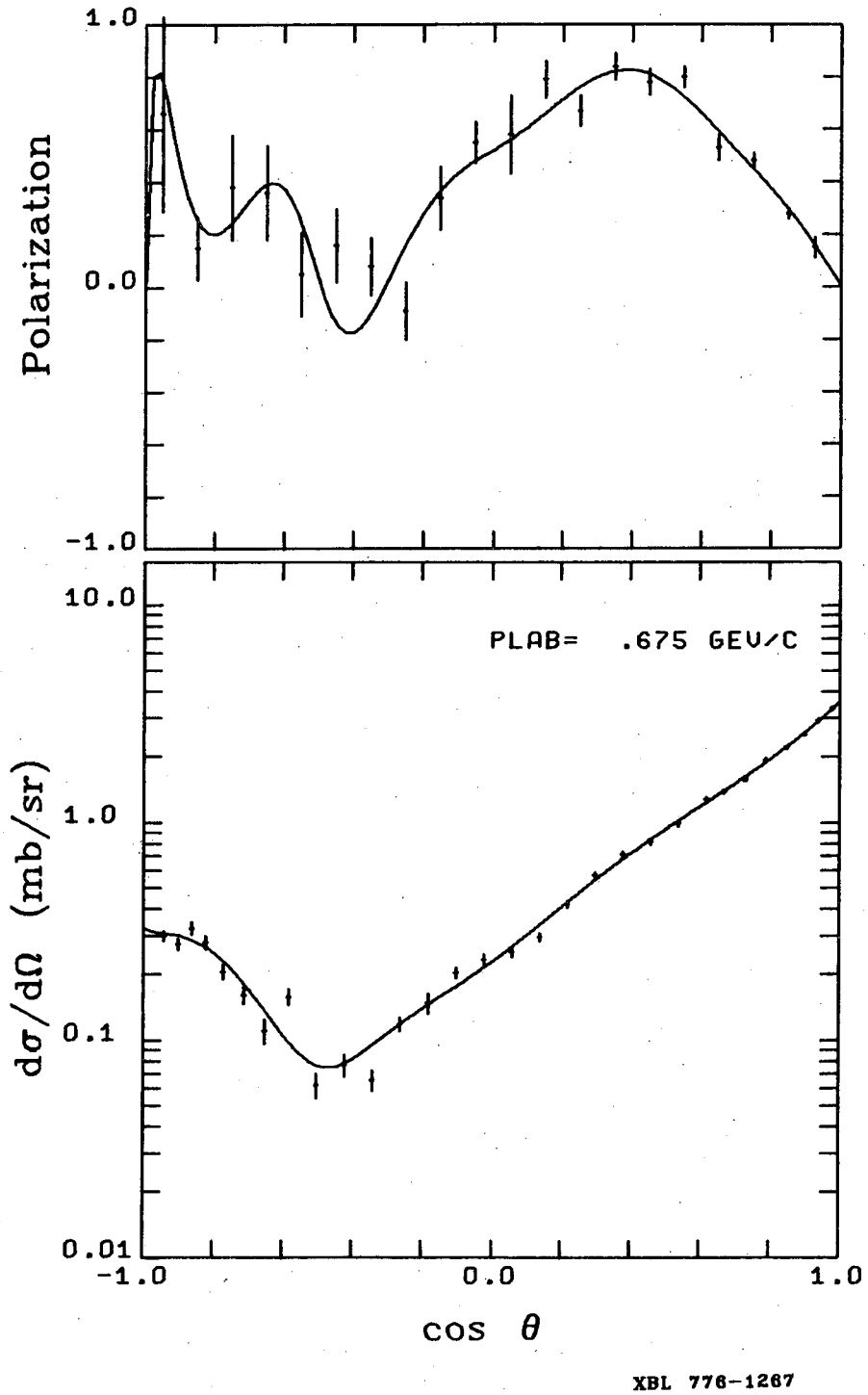
1.0
0.0
-1.0
Polarization
10.0
1.0
0.1
0.01
dσ/dΩ (mb/sr)
PLAB= .675 GEV/C
-1.0
0.0
1.0
cos θ
XBL 776-1267

Figure 7

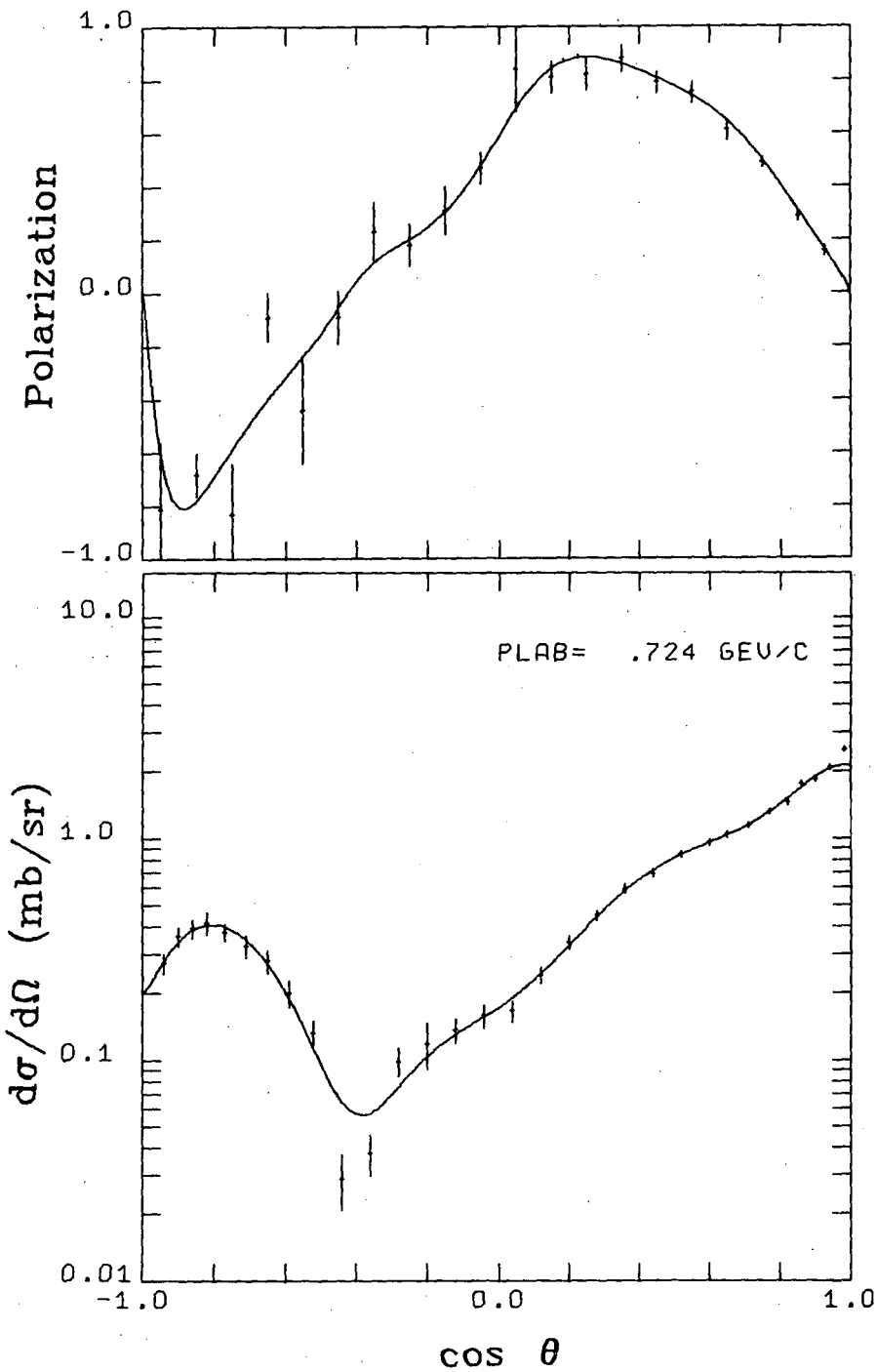

XBL 776-1266

Figure 8

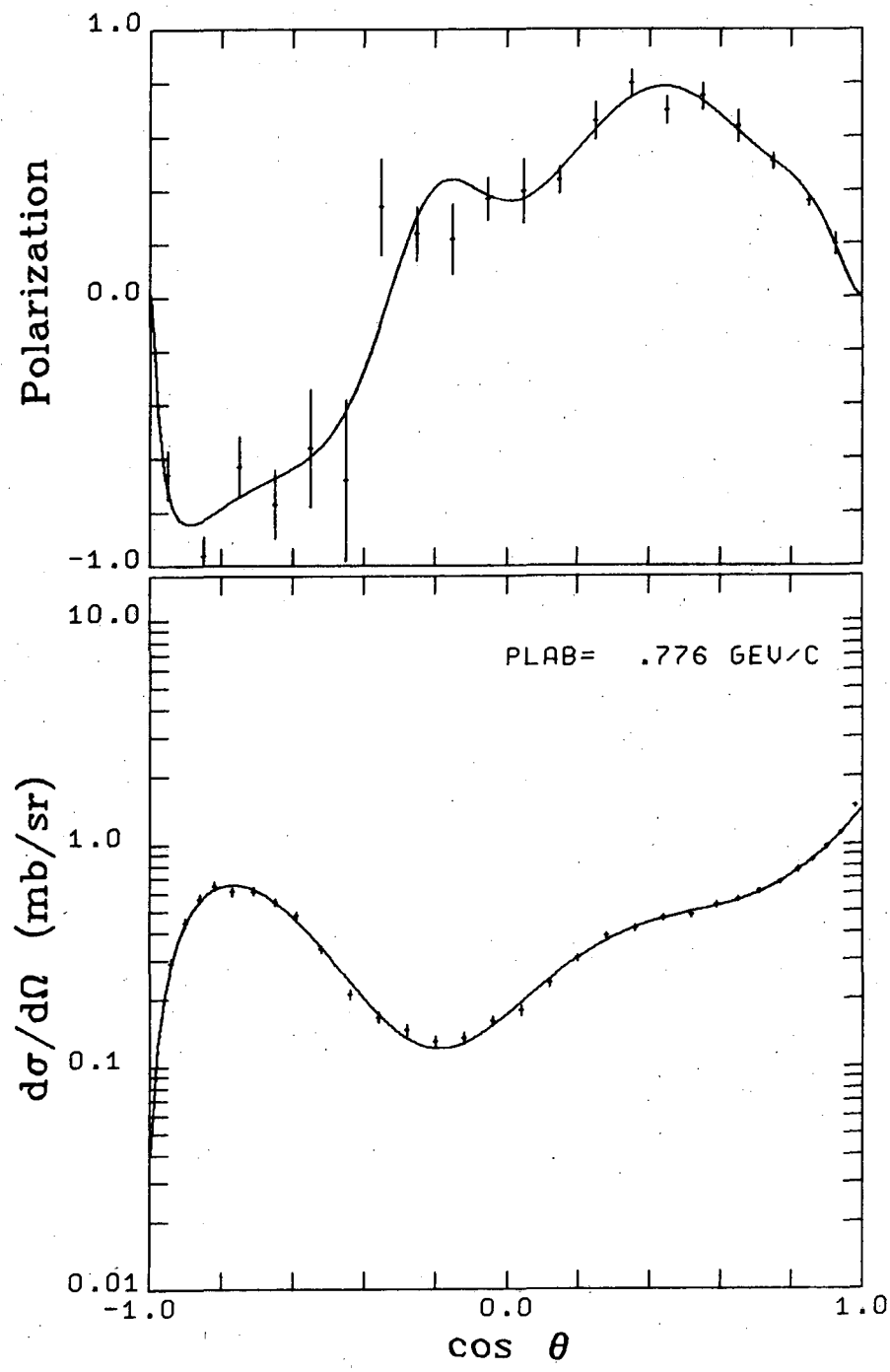

XBL 776-1265

Figure 9

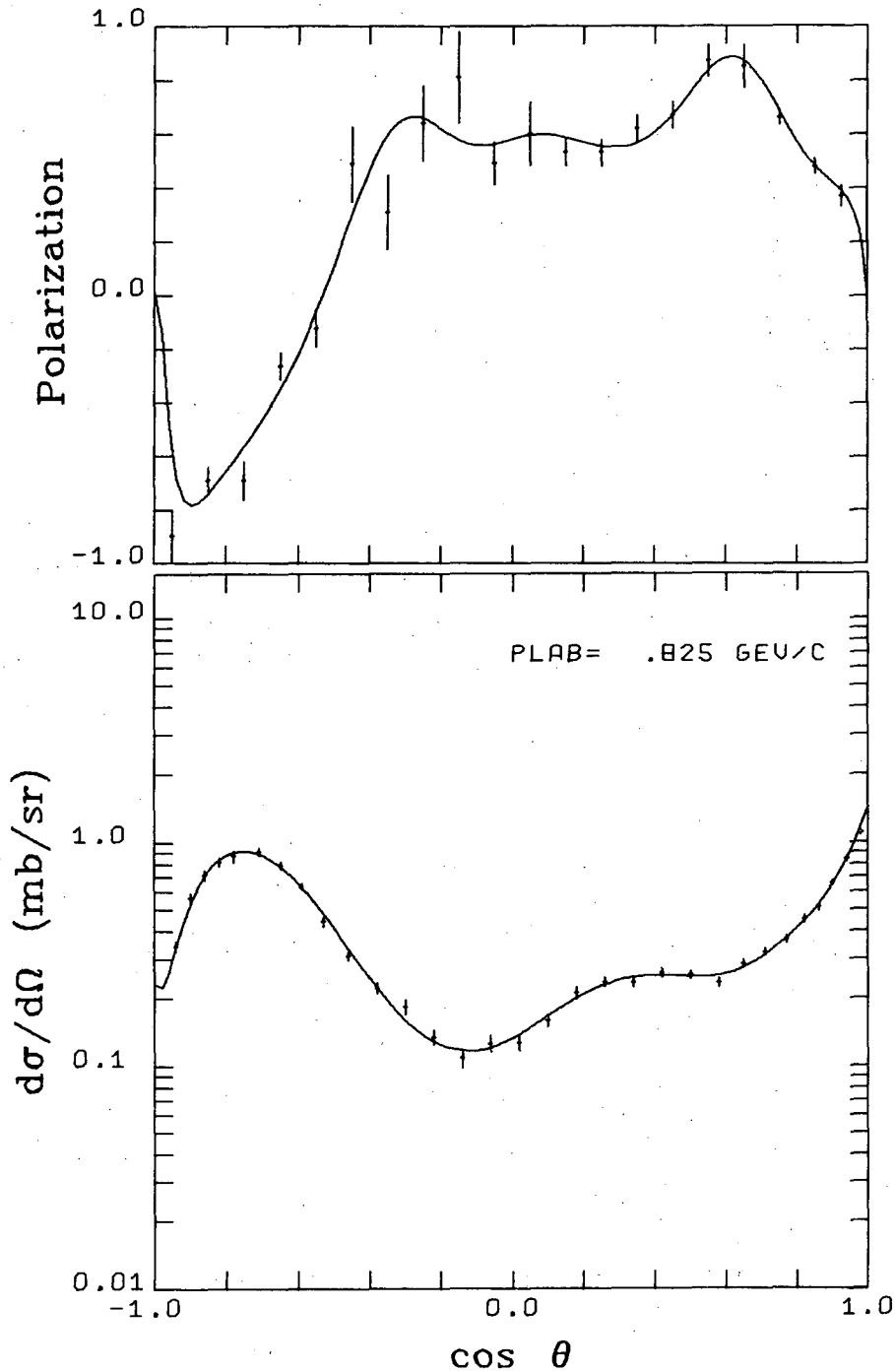

XBL 776-1264

Figure 10

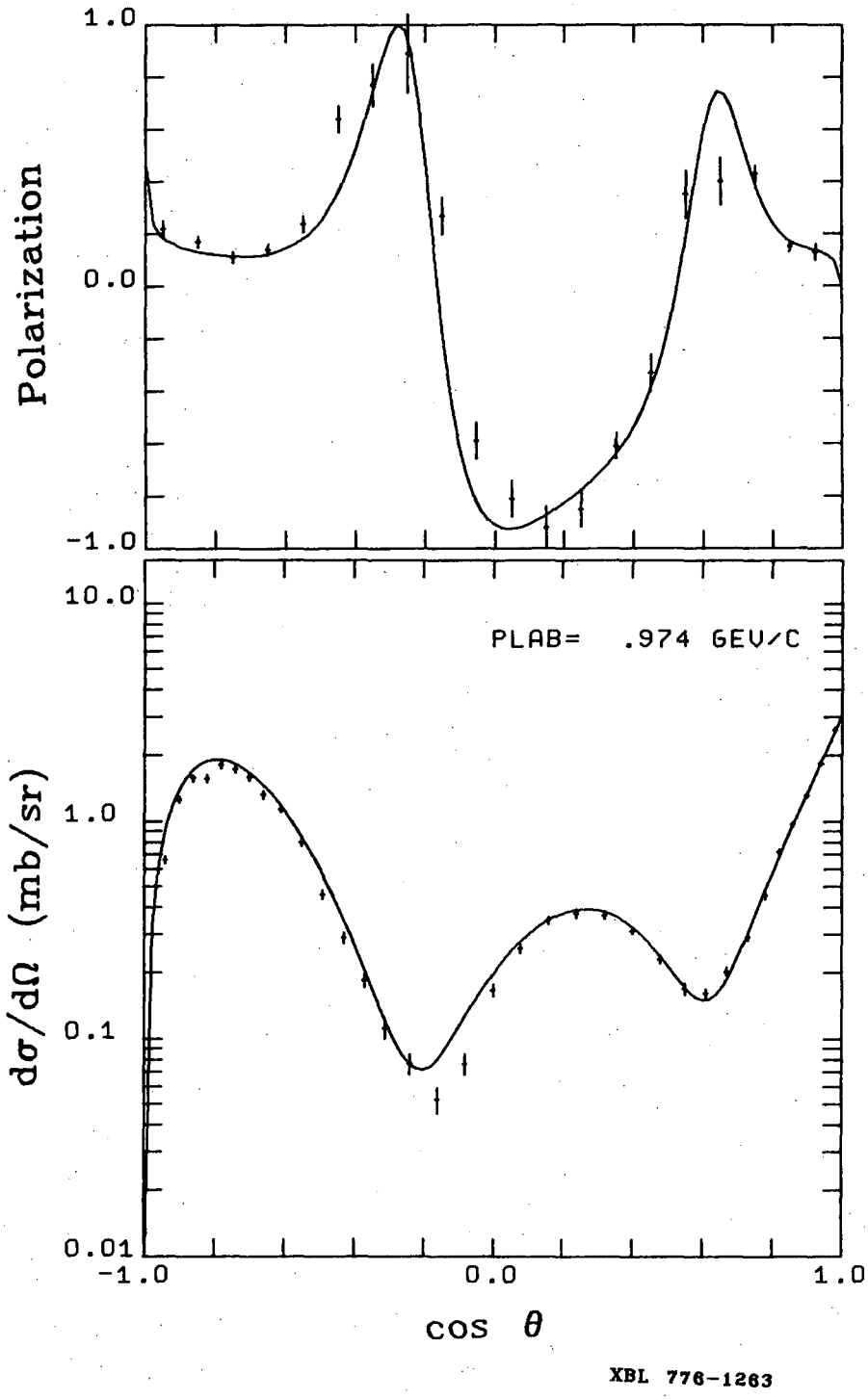
1.0
0.0
-1.0
Polarization
10.0
1.0
0.1
0.01
dσ/dΩ (mb/sr)
PLAB= .974 GEV/C
-1.0
0.0
1.0
cos θ
XBL 776-1263

Figure 11

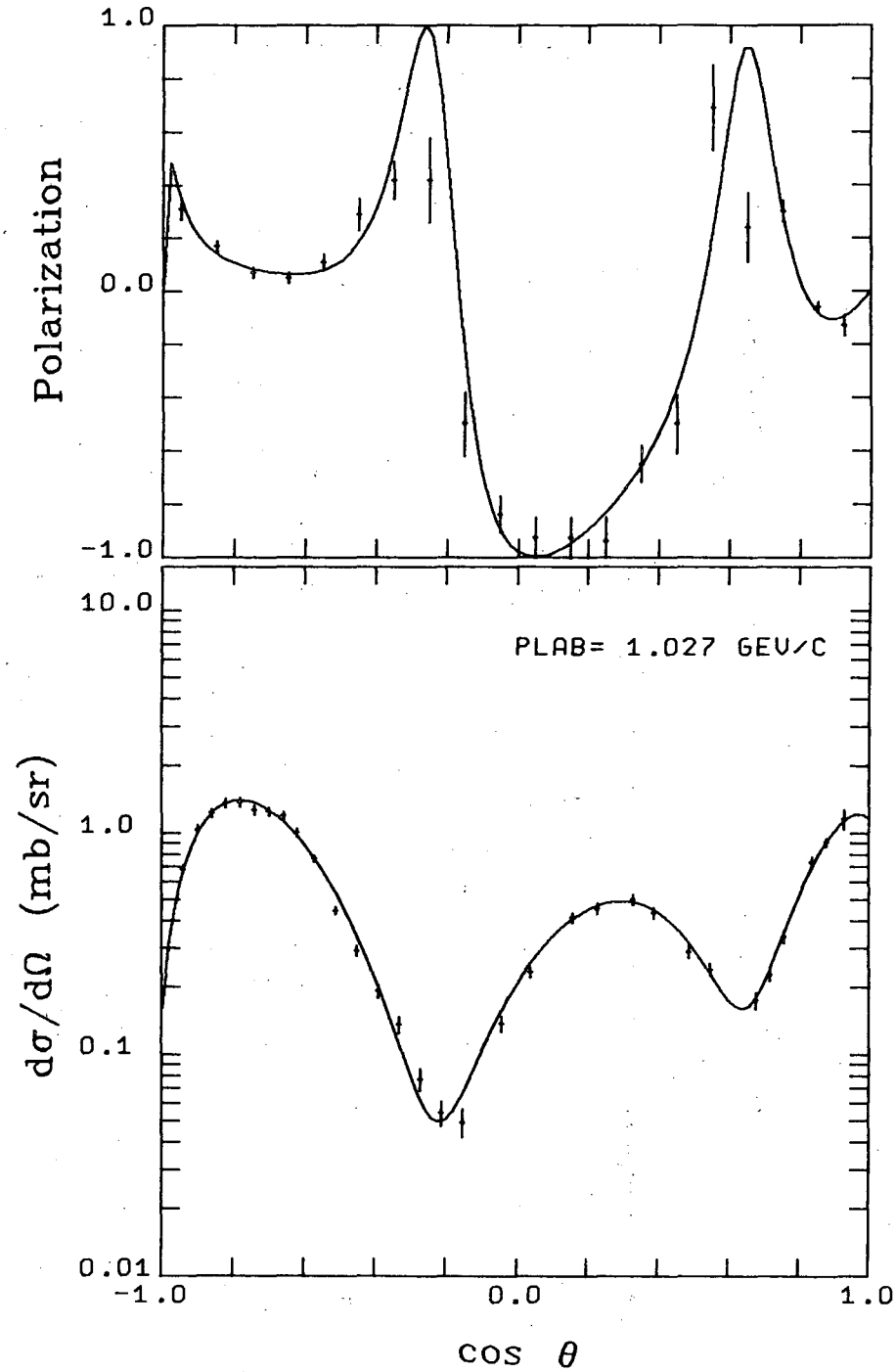

XBL 776-1262

Figure 12

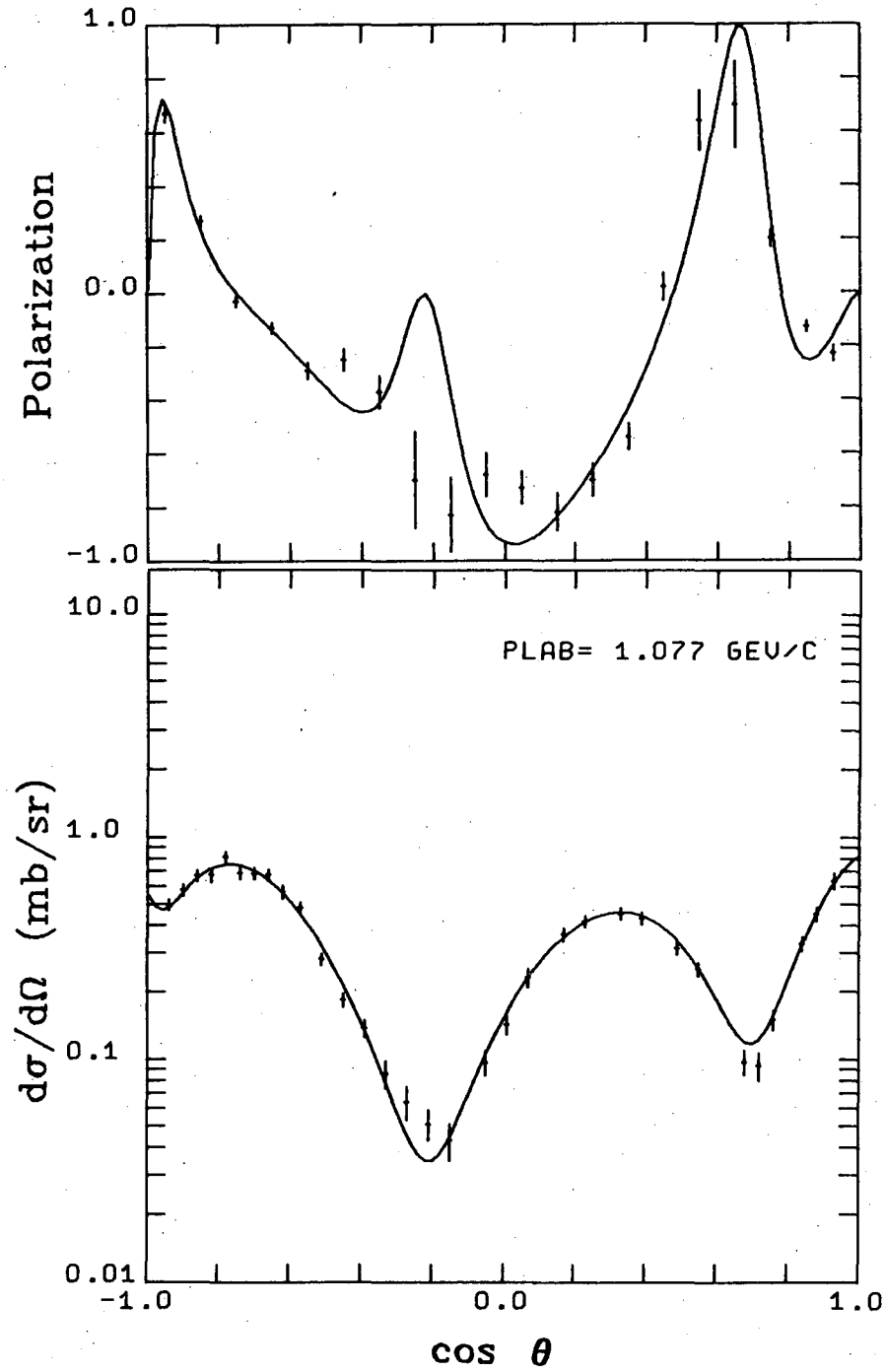

XBL 776-1261

Figure 13

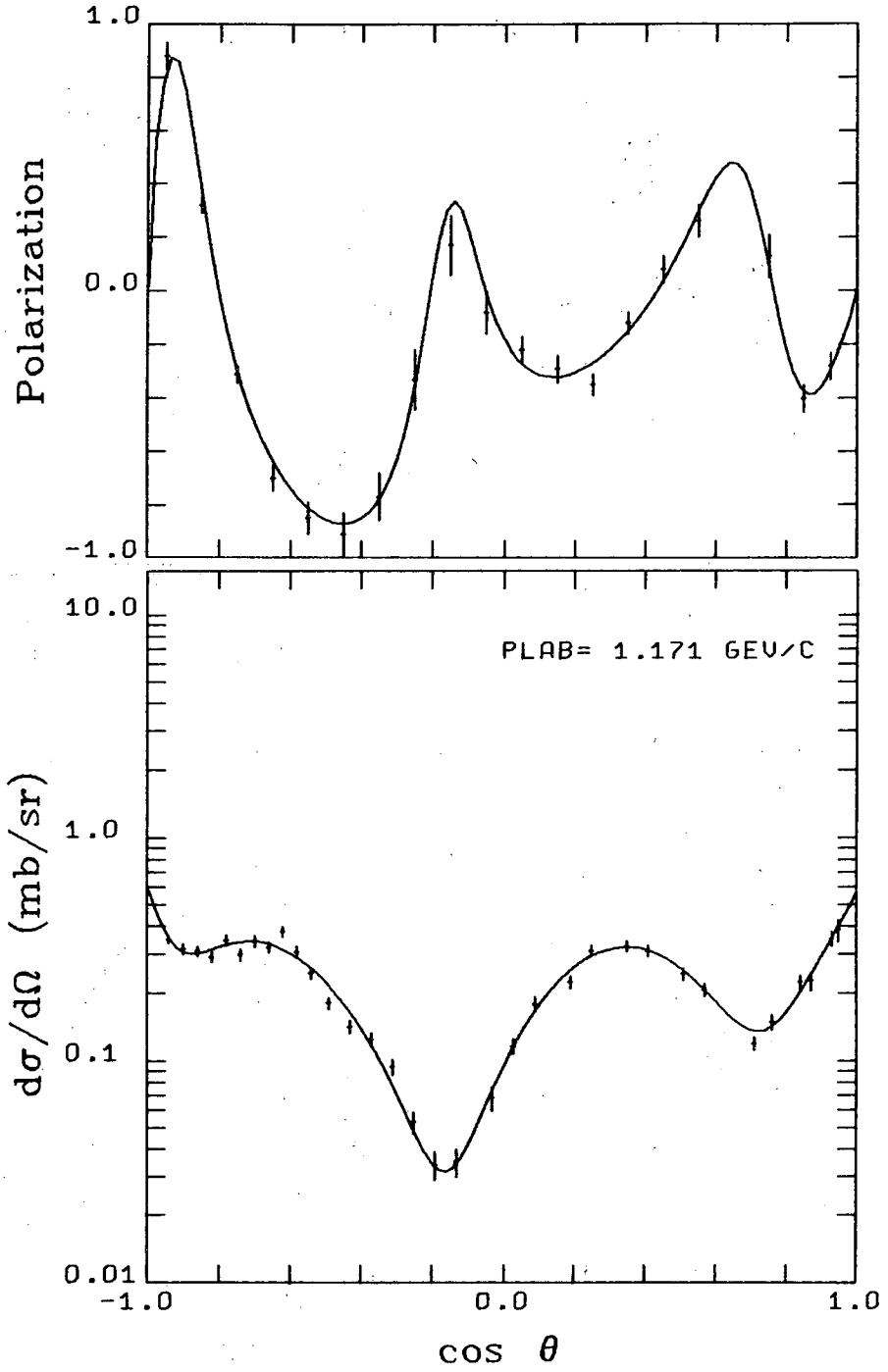

XBL 776-1260

Figure 14

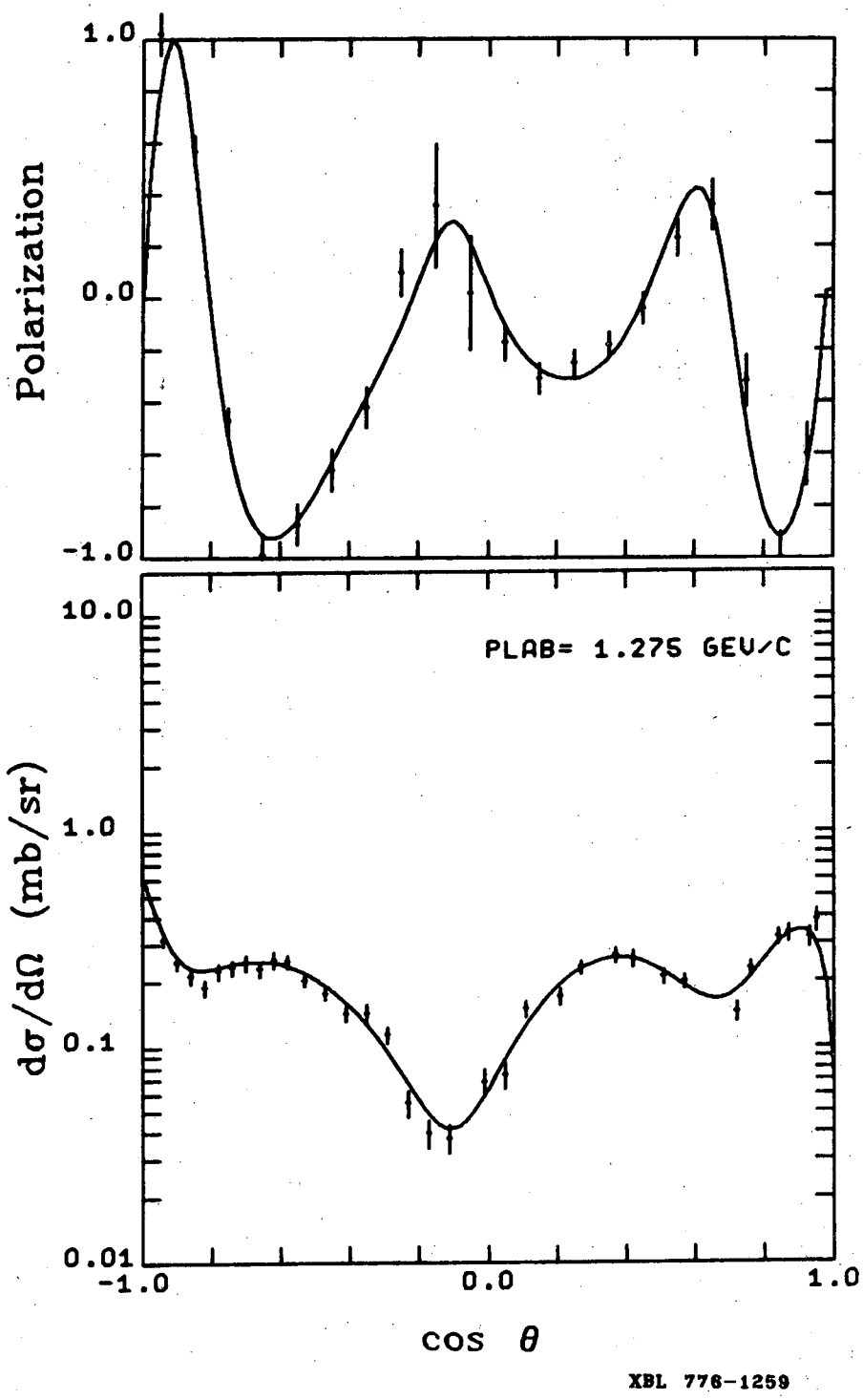
1.0
0.0
-1.0
Polarization
10.0
1.0
0.1
0.01
dσ/dΩ (mb/sr)
PLAB= 1.275 GEV/C
-1.0
0.0
1.0
cos θ
XBL 776-1259

Figure 15

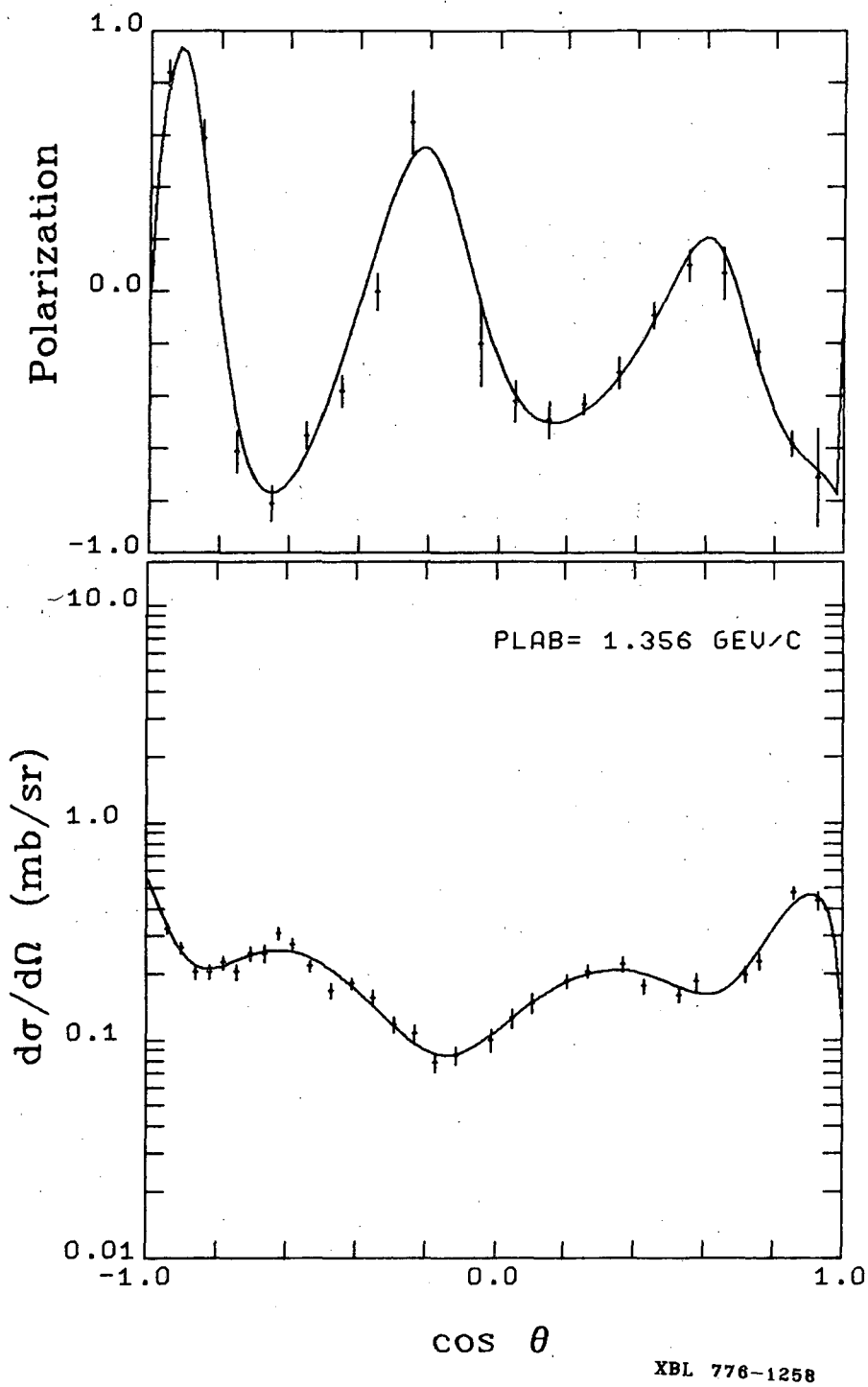
1.0
0.0
-1.0
Polarization
10.0
1.0
0.1
0.01
dσ/dΩ (mb/sr)
PLAB= 1.356 GEV/C
-1.0
0.0
1.0
cos θ
XBL 776-1258

Figure 16

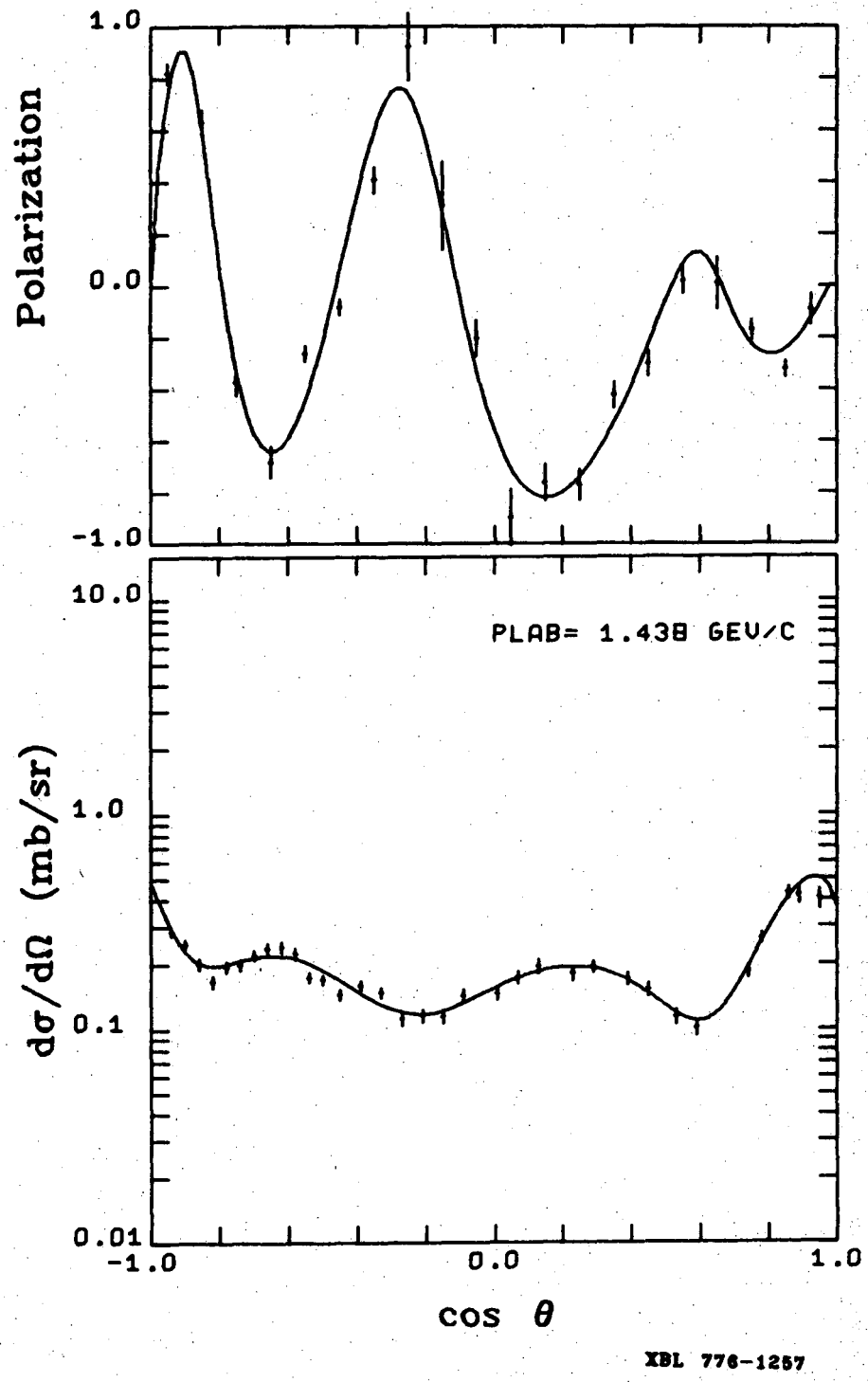
1.0
0.0
-1.0
Polarization
10.0
1.0
0.1
0.01
dσ/dΩ (mb/sr)
PLAB= 1.438 GEV/C
-1.0
0.0
1.0
cos θ
XBL 776-1257

Figure 17

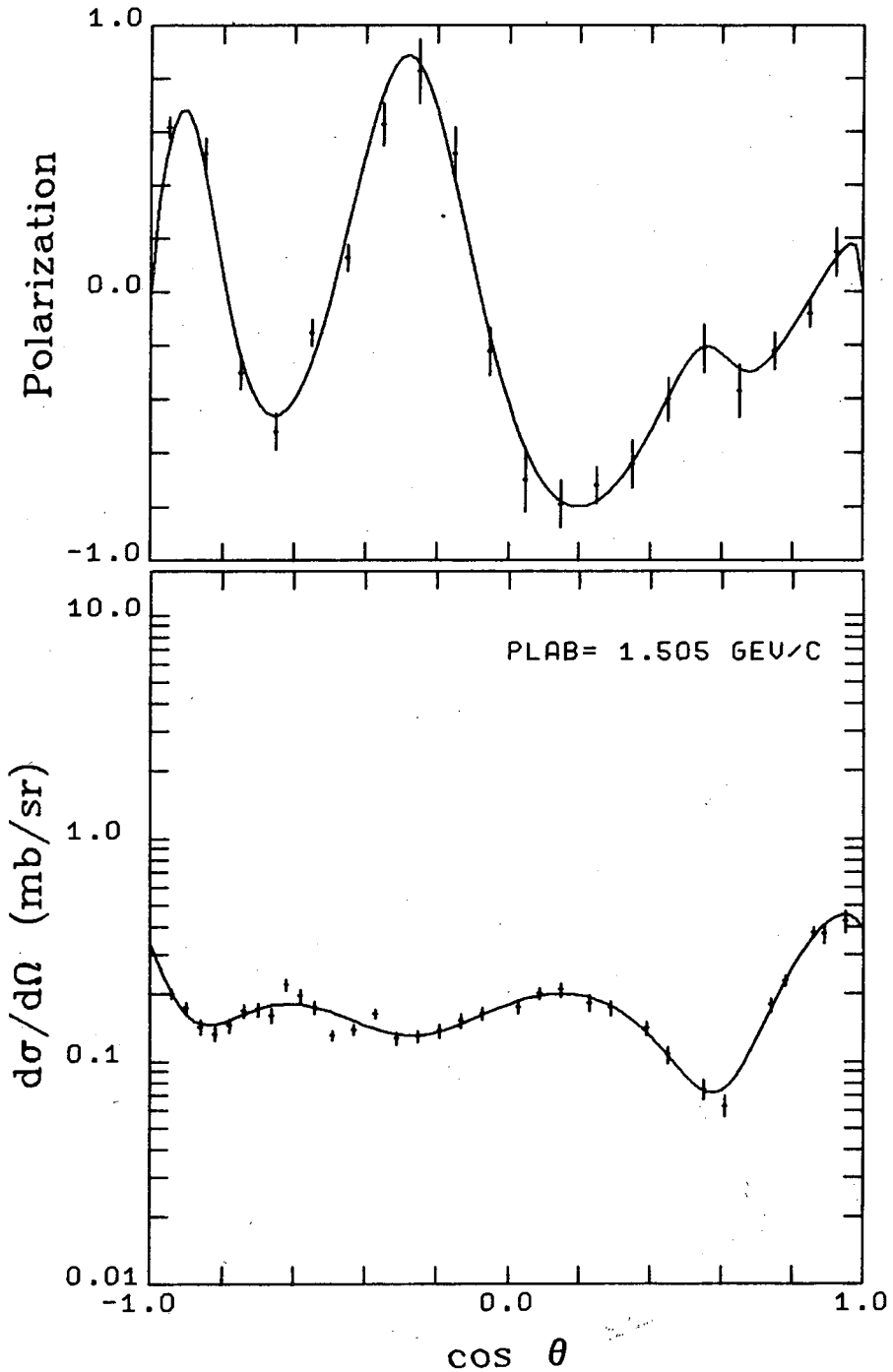

XBL 776-1256

Figure 18

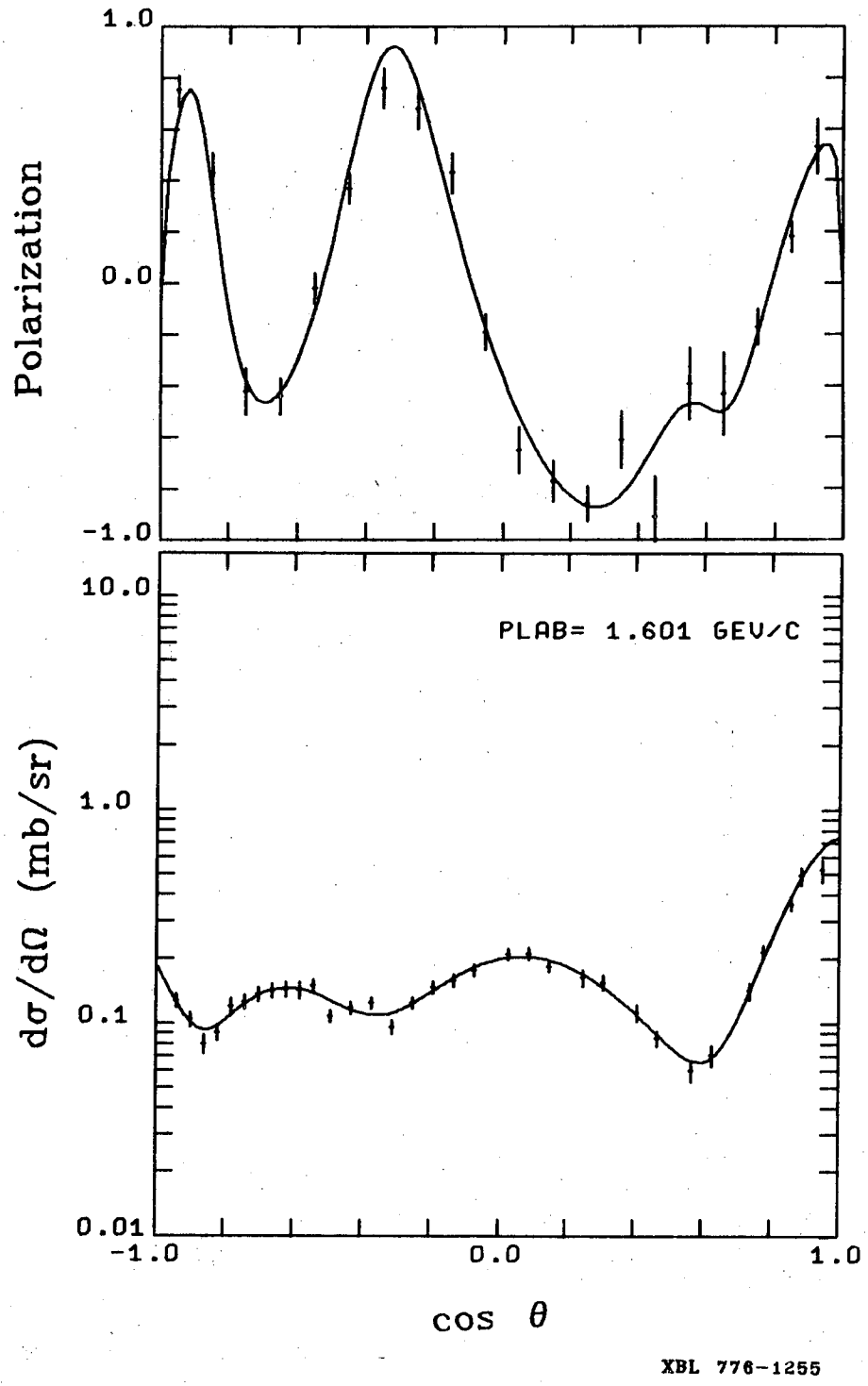
1.0
0.0
-1.0
Polarization
10.0
1.0
0.1
0.01
dσ/dΩ (mb/sr)
PLAB= 1.601 GEV/C
-1.0
0.0
1.0
cos θ
XBL 776-1255

Figure 19

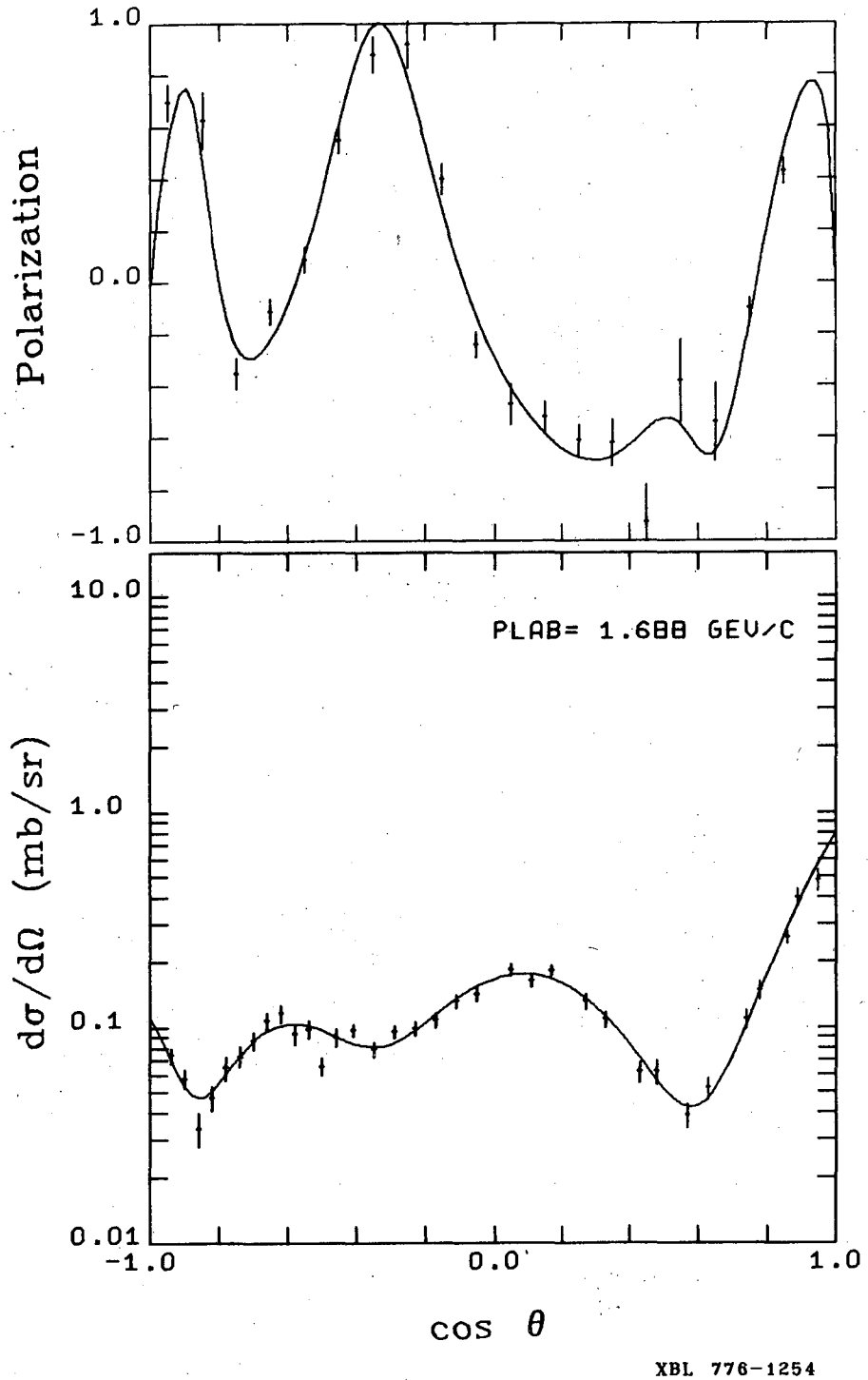
1.0
0.0
-1.0
Polarization
10.0
1.0
0.1
0.01
dσ/dΩ (mb/sr)
PLAB= 1.688 GEV/C
-1.0
0.0
1.0
cos θ
XBL 776-1254

Figure 20

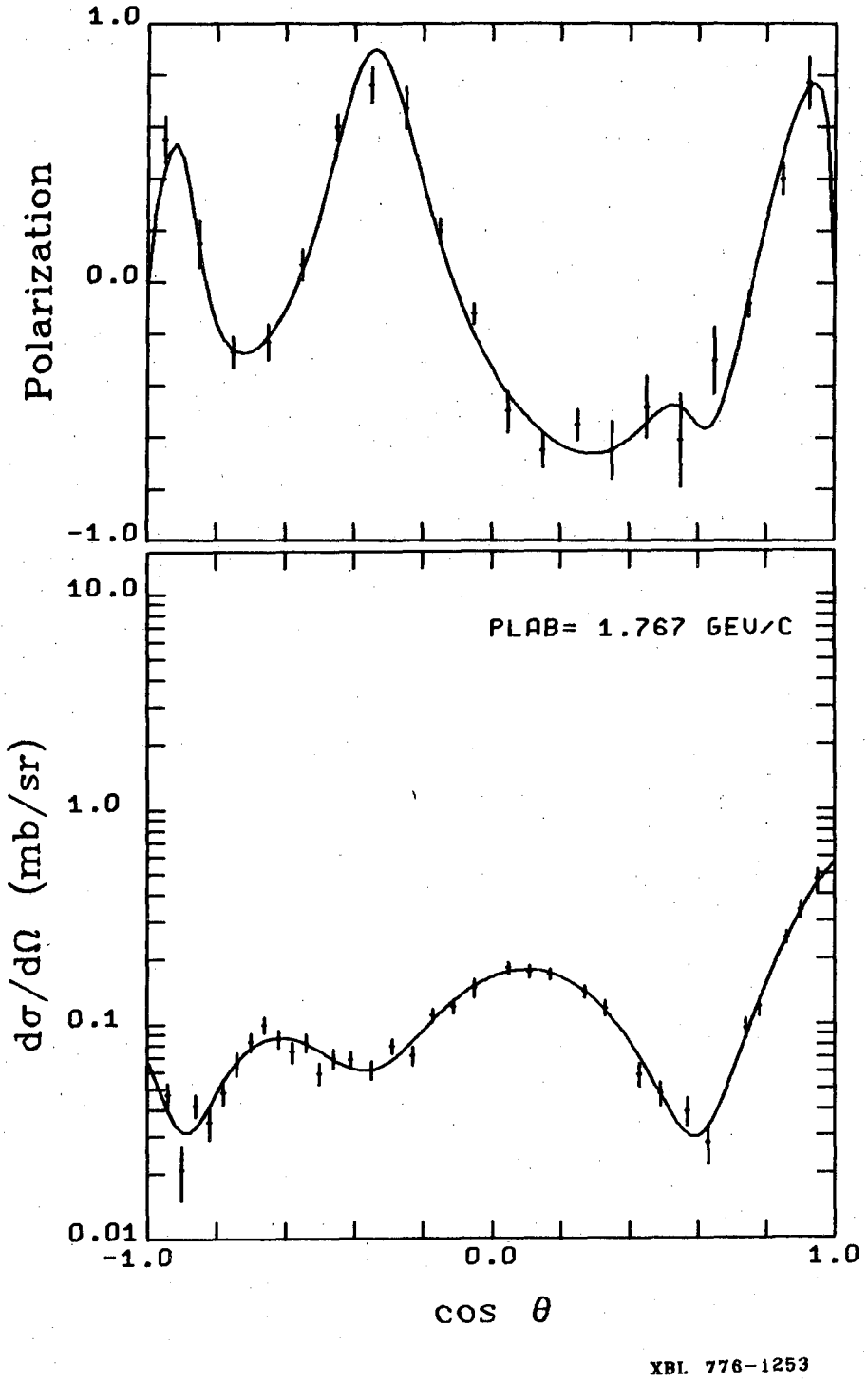
1.0
0.0
-1.0
Polarization
10.0
1.0
0.1
0.01
dσ/dΩ (mb/sr)
PLAB= 1.767 GEV/C
-1.0
0.0
1.0
cos θ
XBL 776-1253

Figure 21

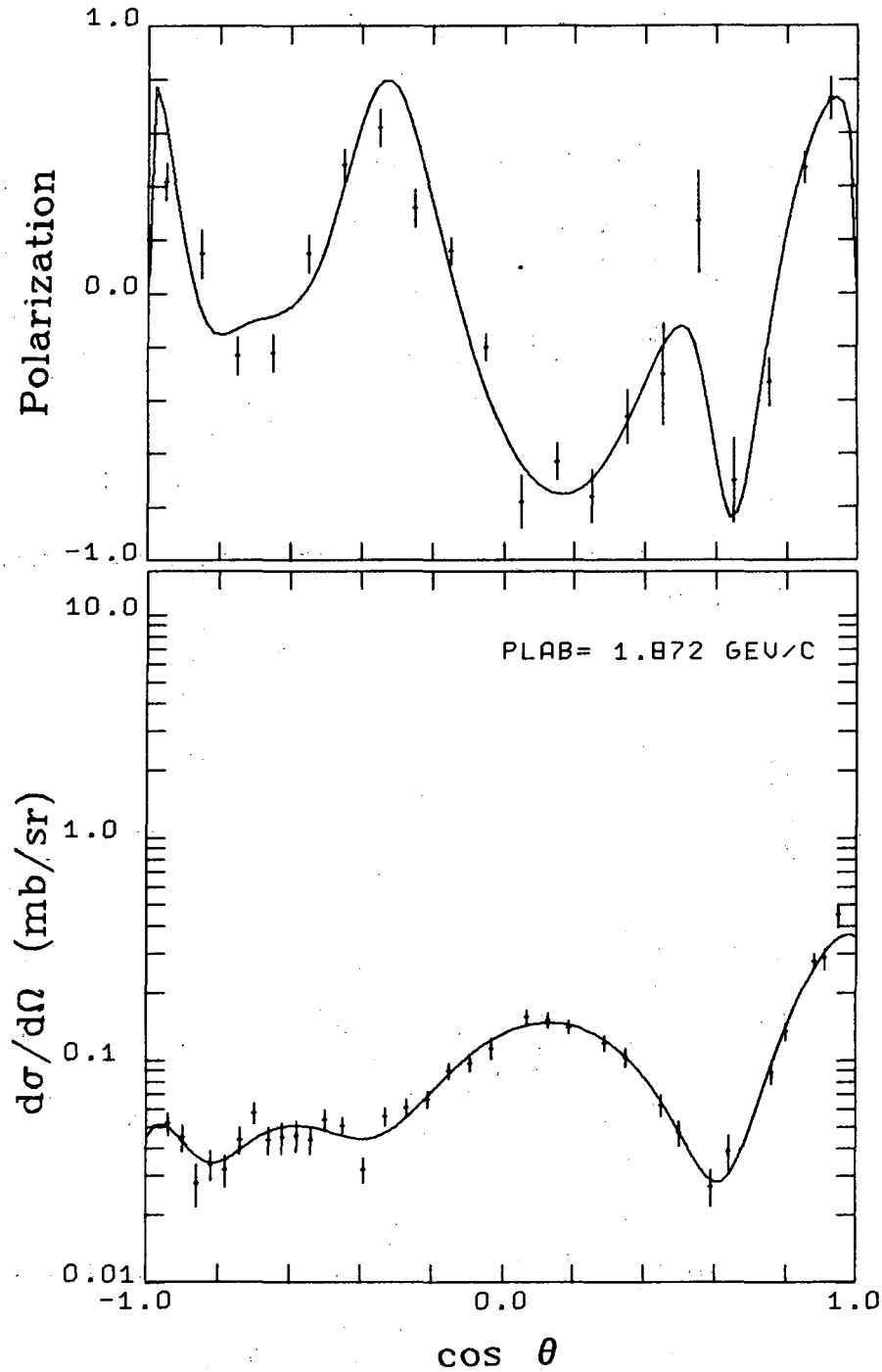

XBL 776-1252

Figure 22

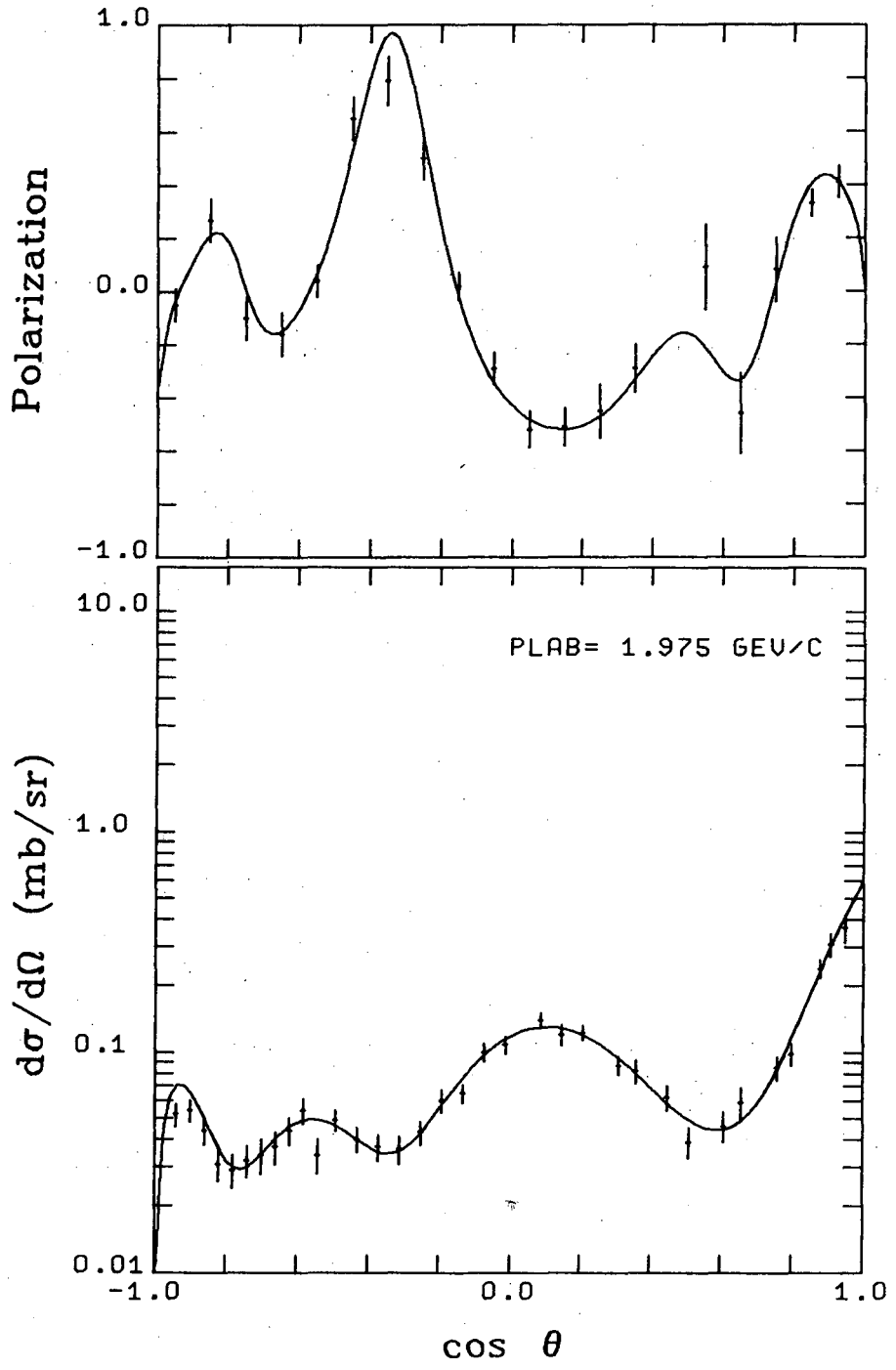

XBL 776-1251

Figure 23

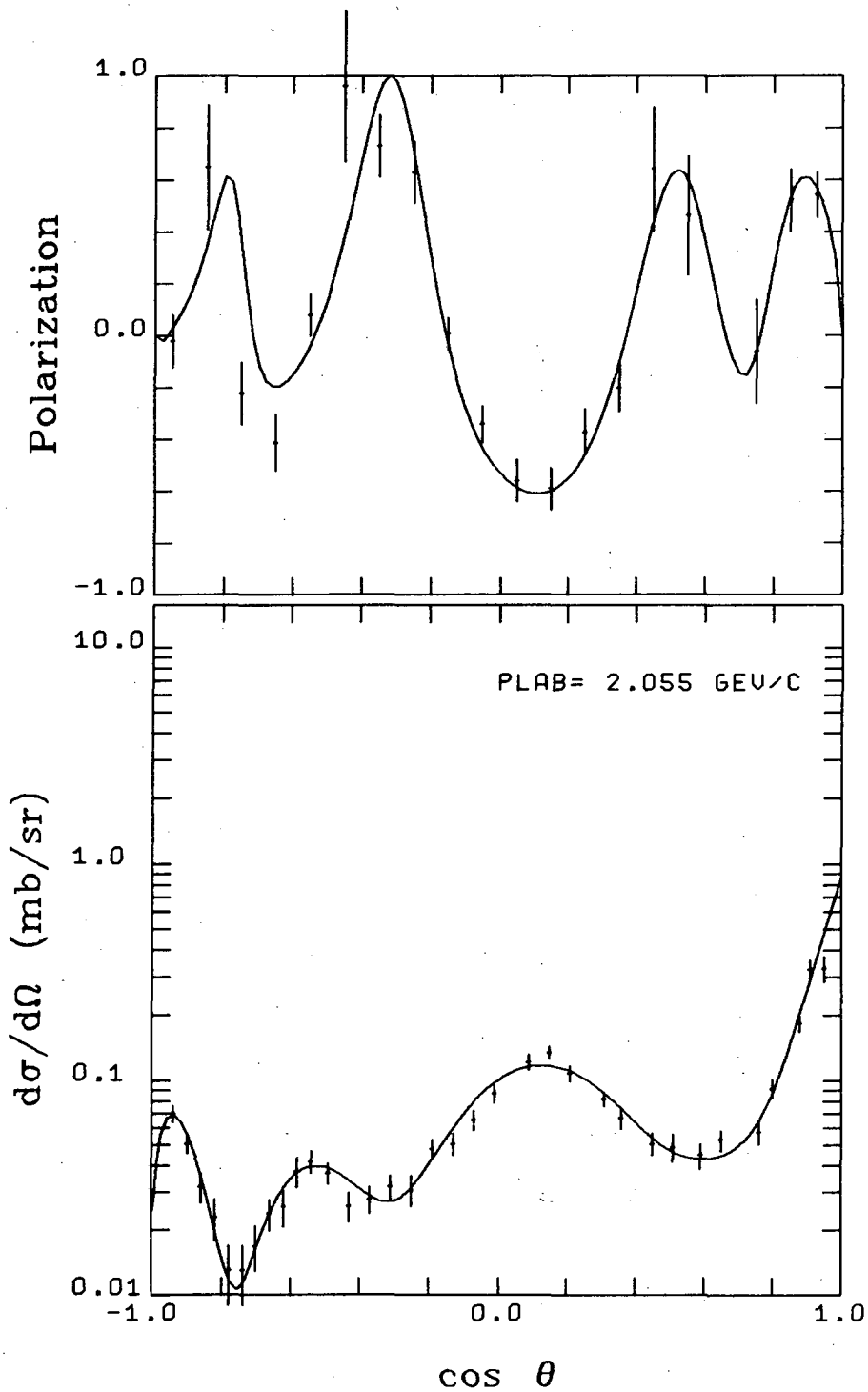

XBL 776-1250

Figure 24

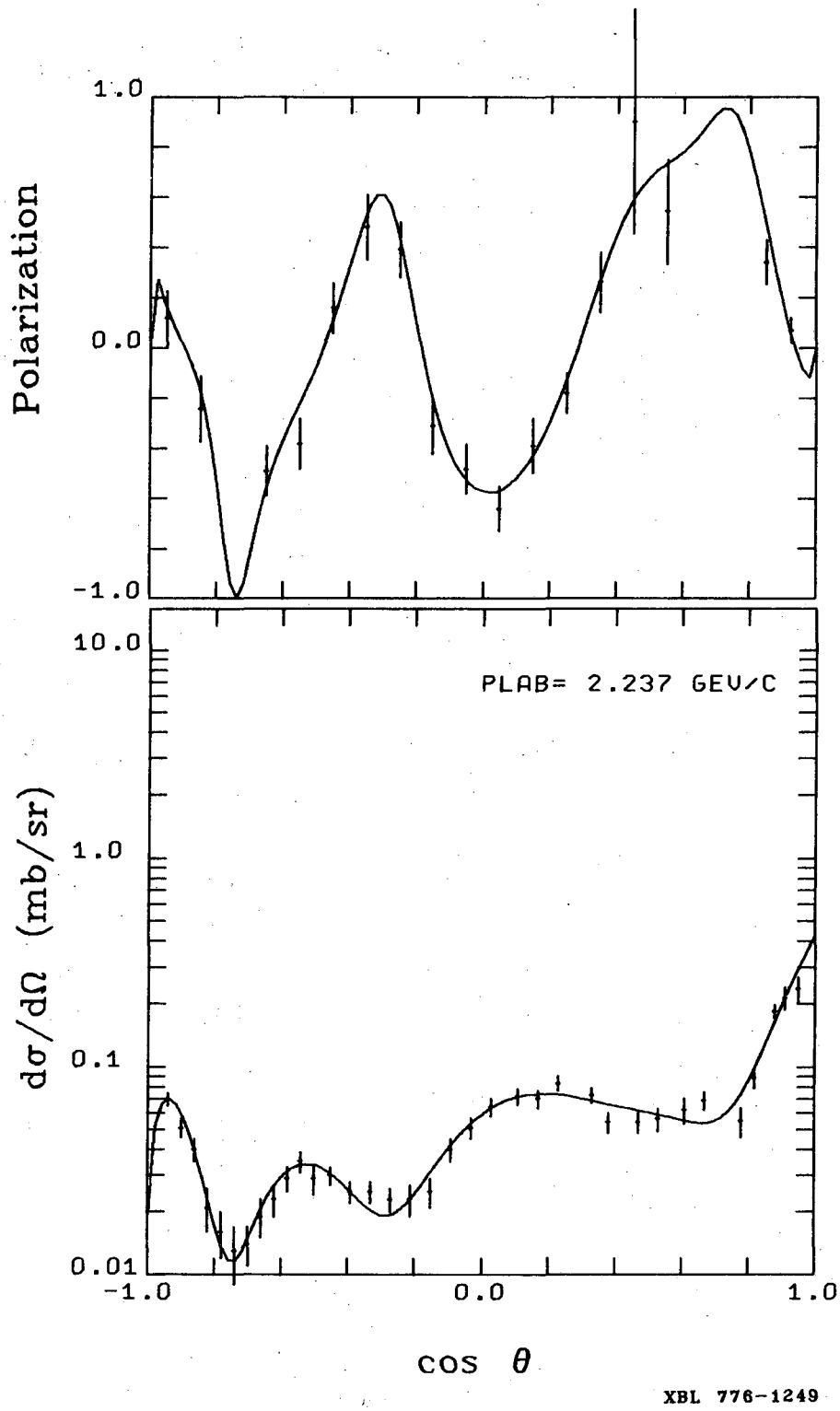
1.0
0.0
-1.0
Polarization
10.0
1.0
0.1
0.01
dσ/dΩ (mb/sr)
PLAB= 2.237 GEV/C
-1.0
0.0
1.0
cos θ
XBL 776-1249

Figure 25

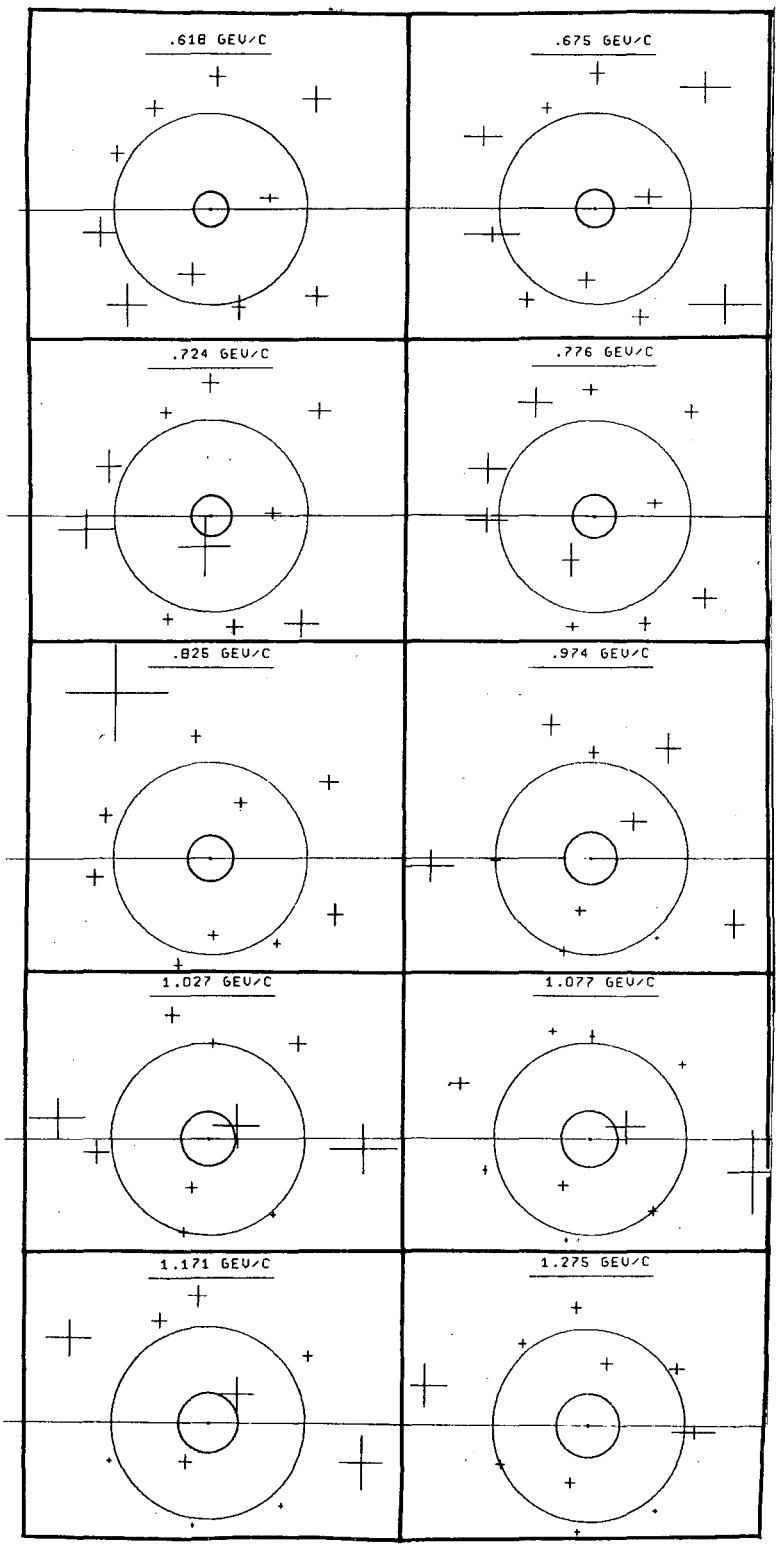

XBL 778-2551A

Figure 26 (a)

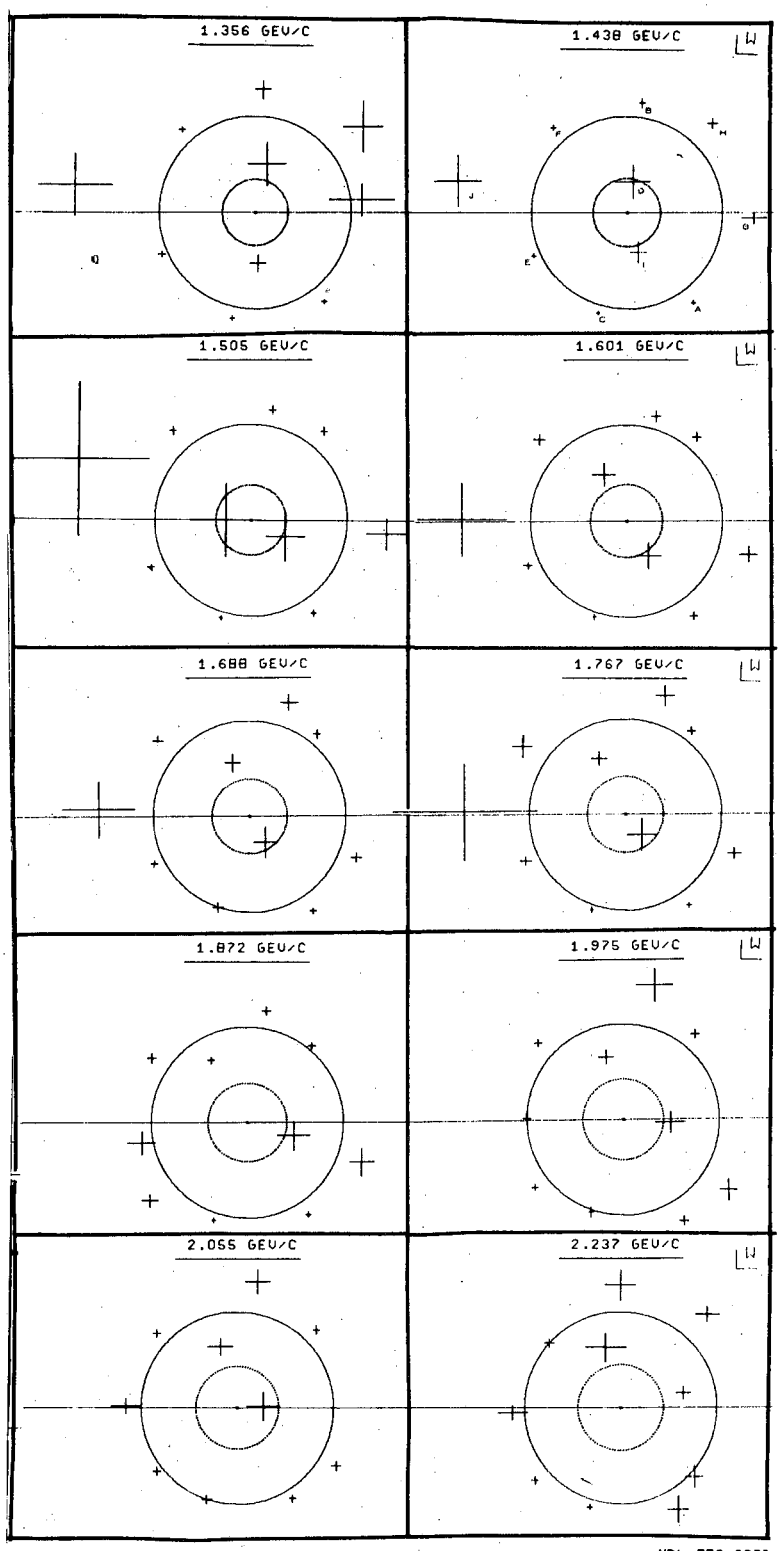

XBL 778-2551

Figure 26 (b)

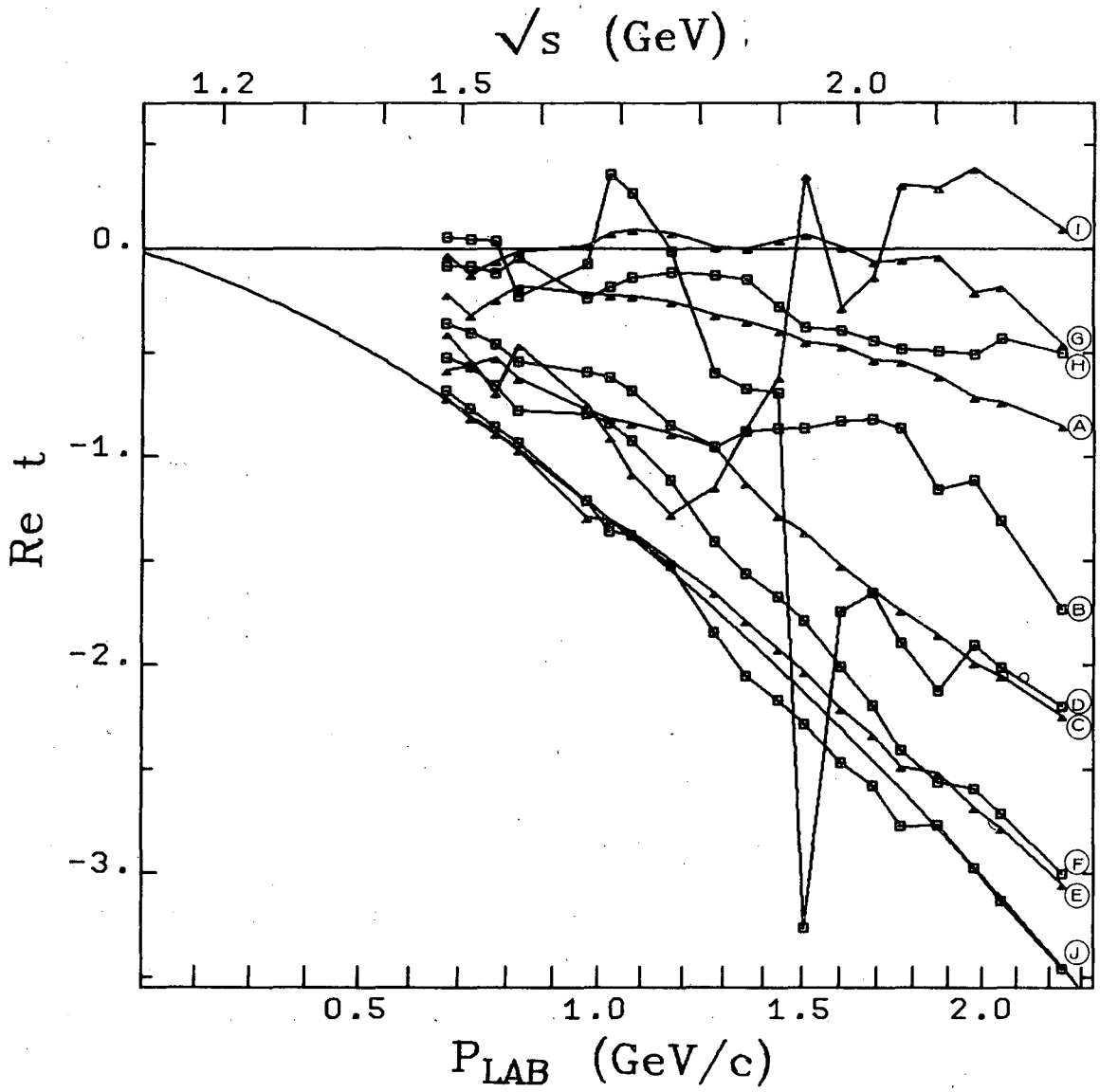

XBL 776-1242

Figure 27

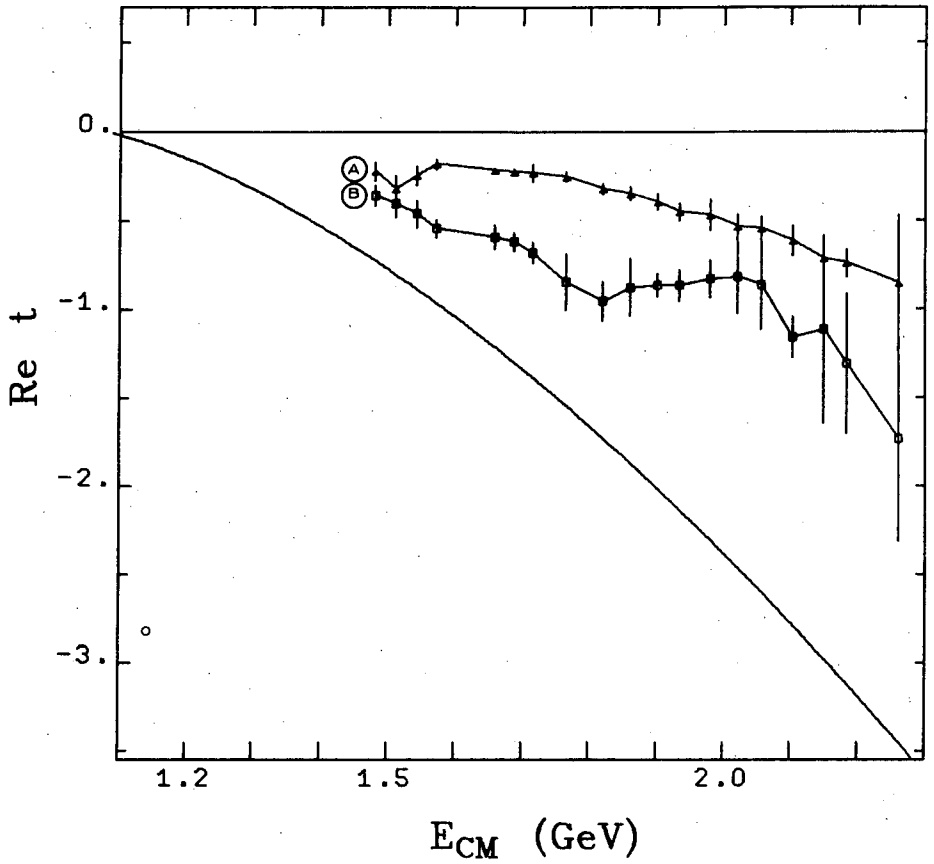

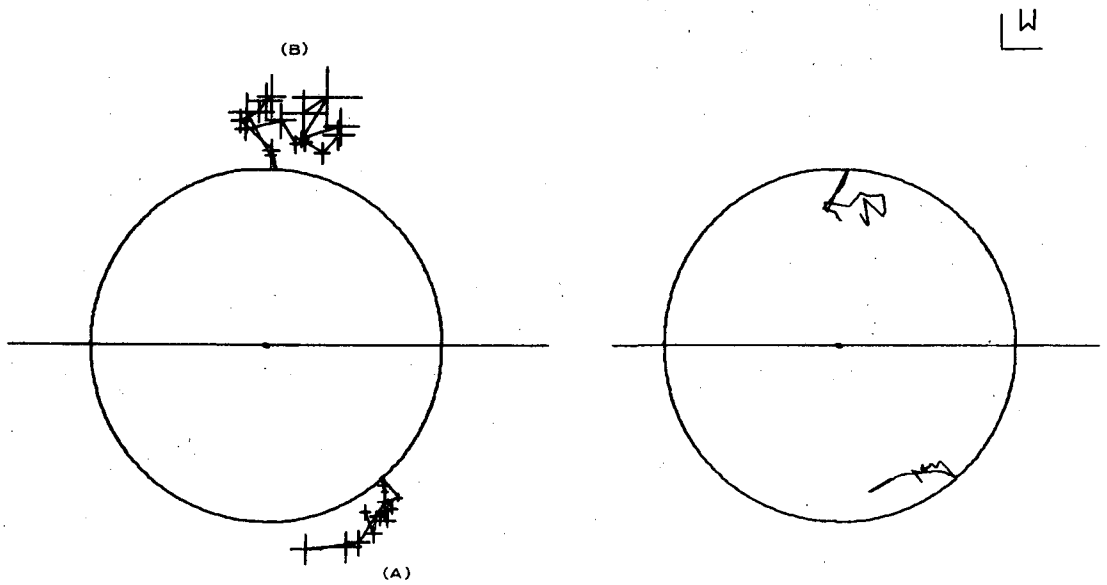

XBL 776-1244

Figure 28

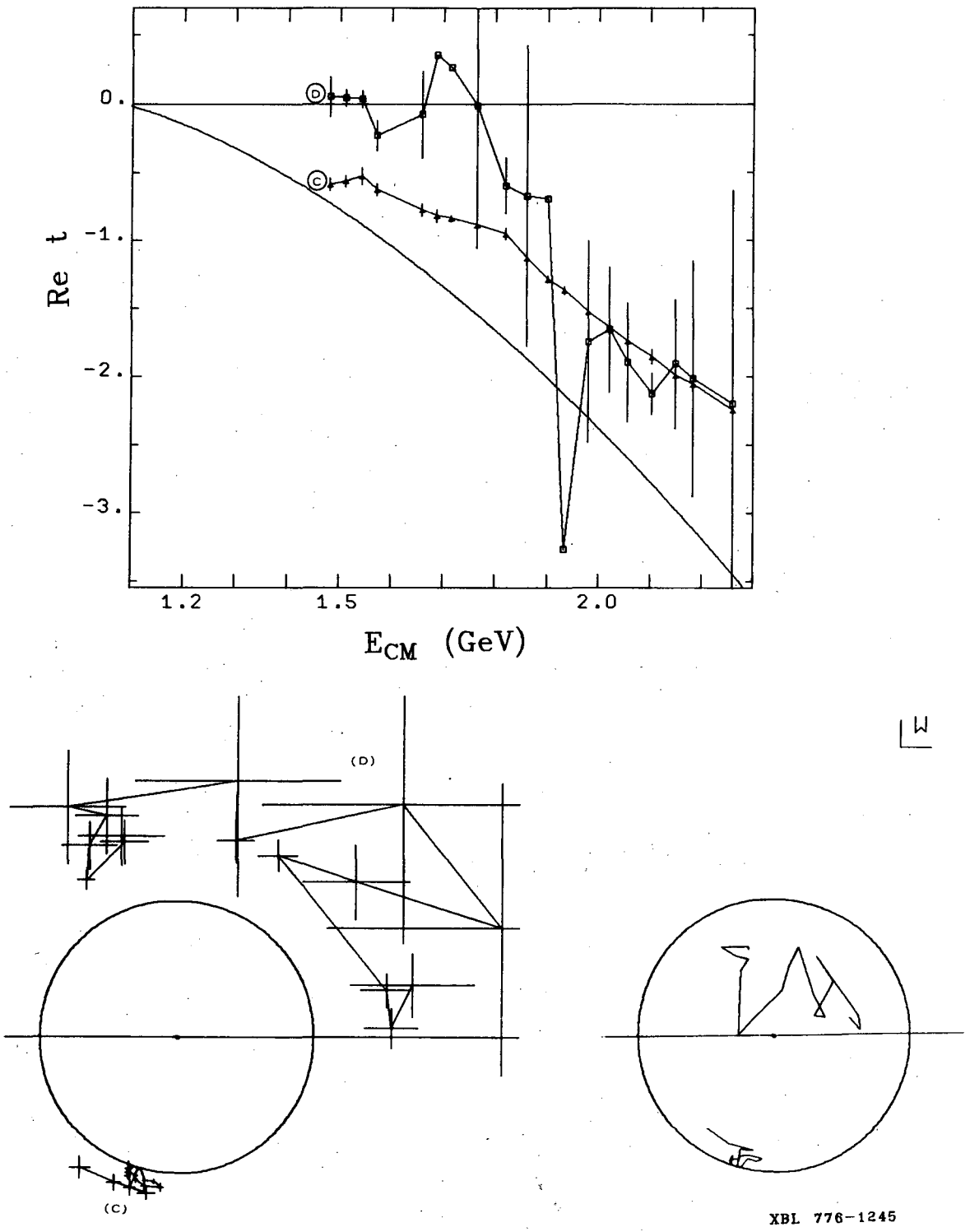

Figure 29

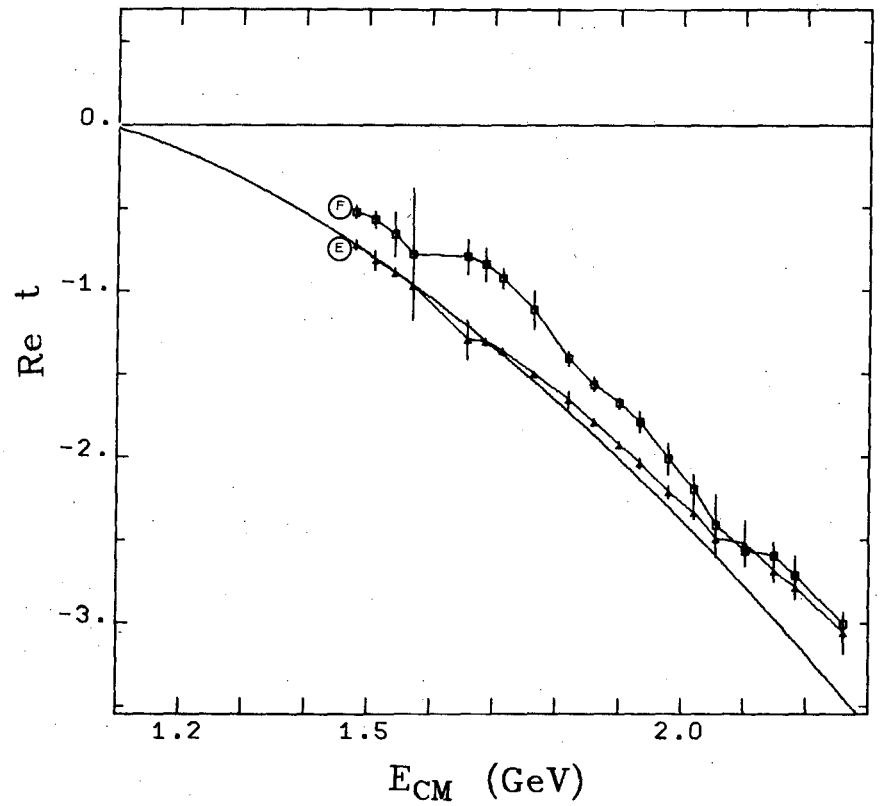

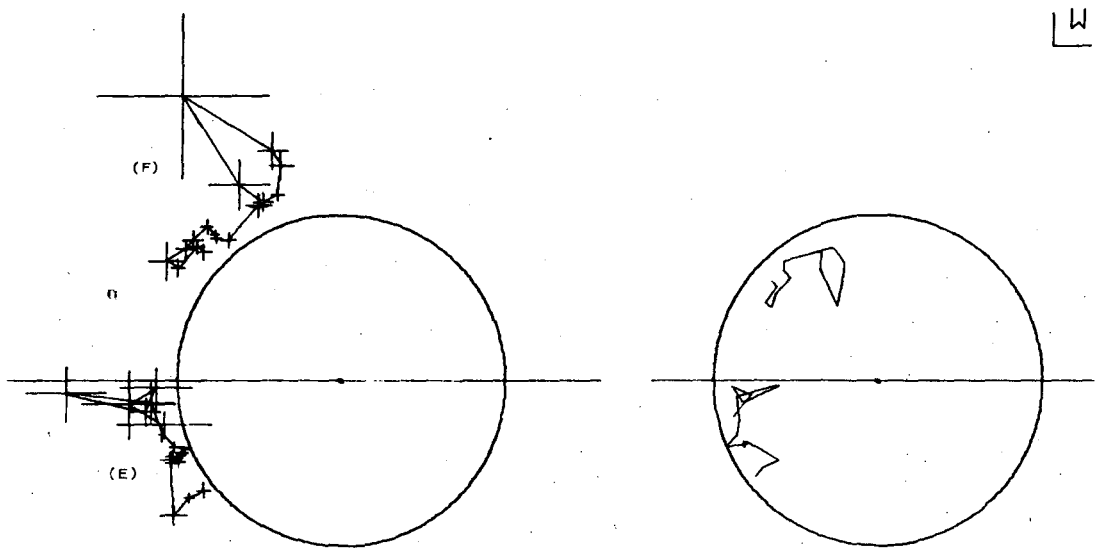

XBL 776-1246

Figure 30

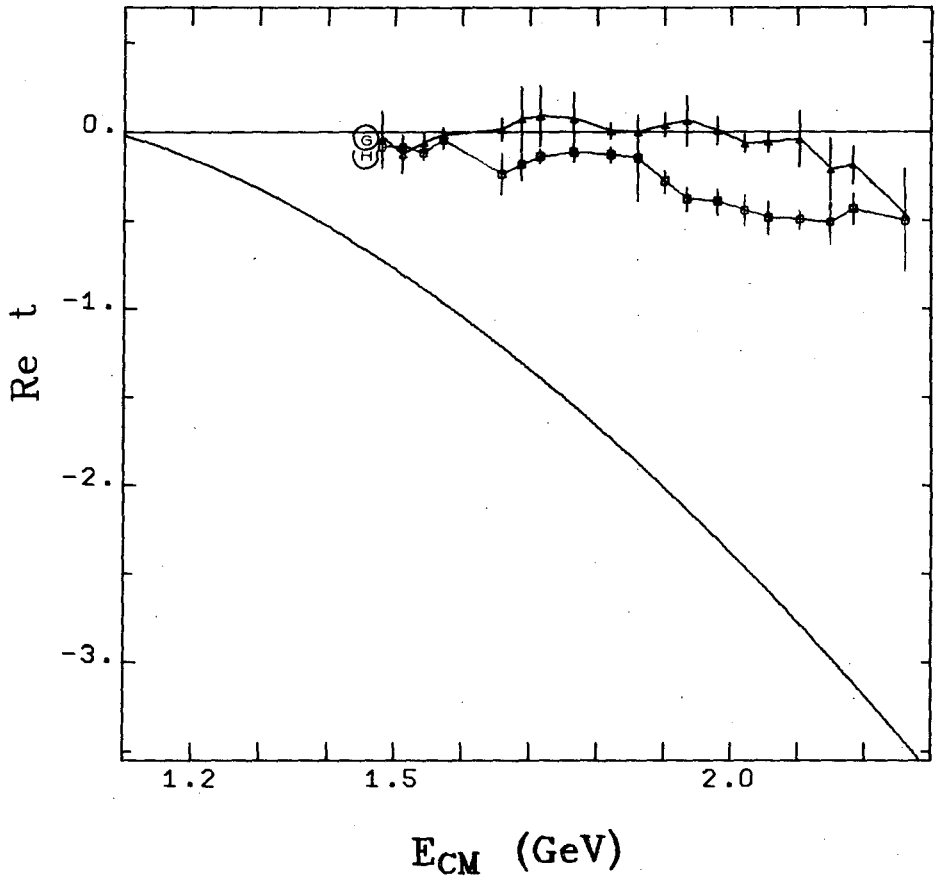

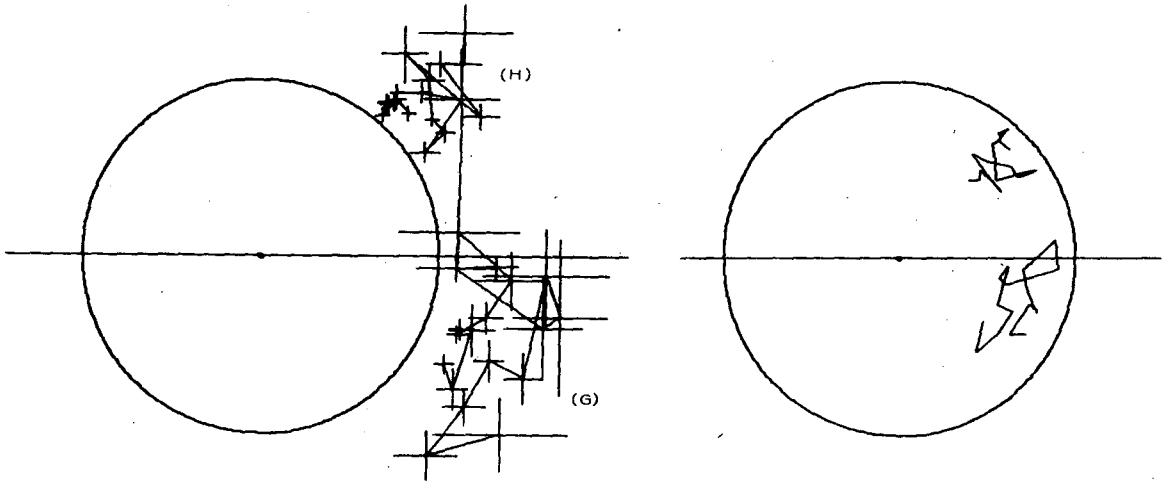

XBL 776-1247

Figure 31

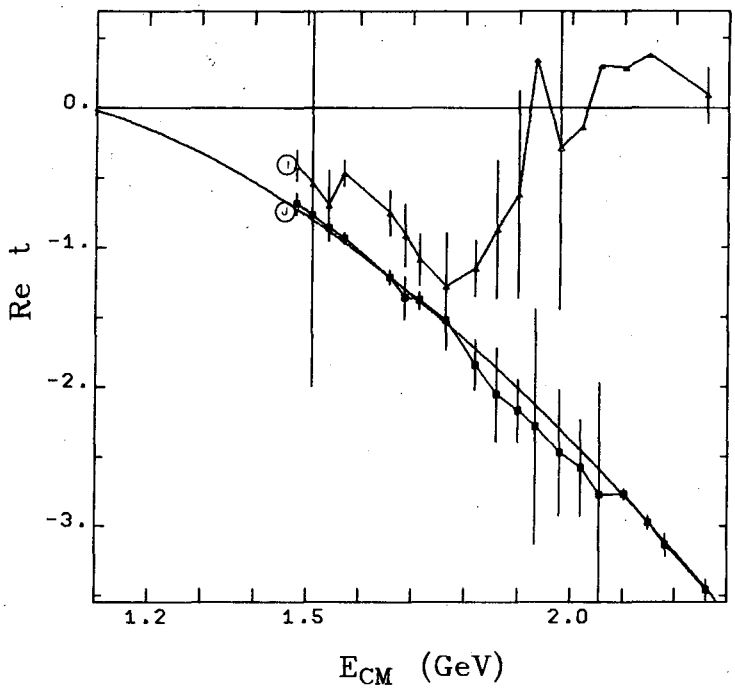

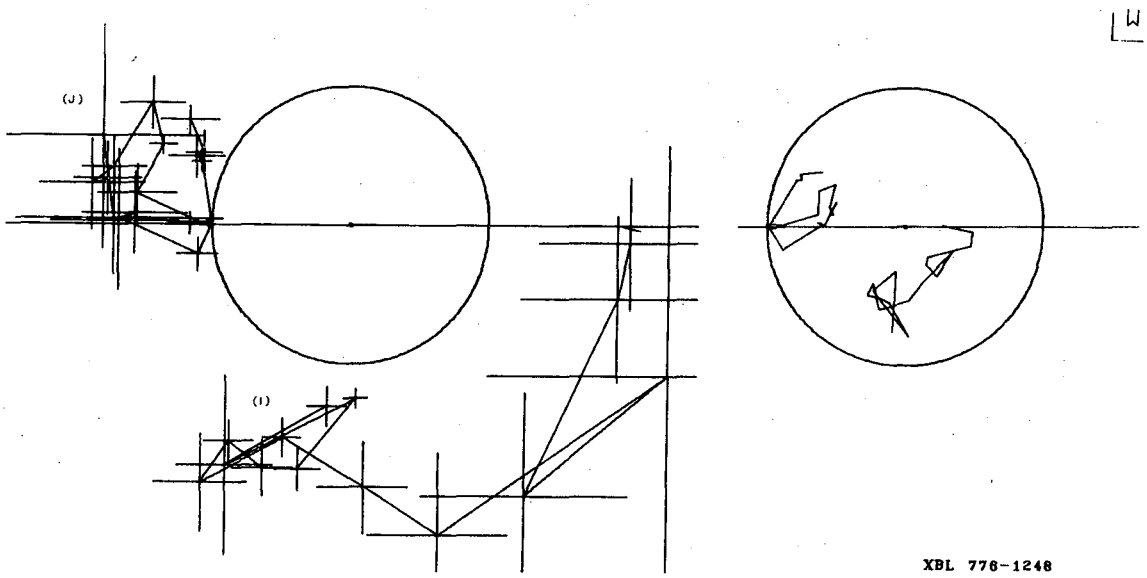

Figure 32

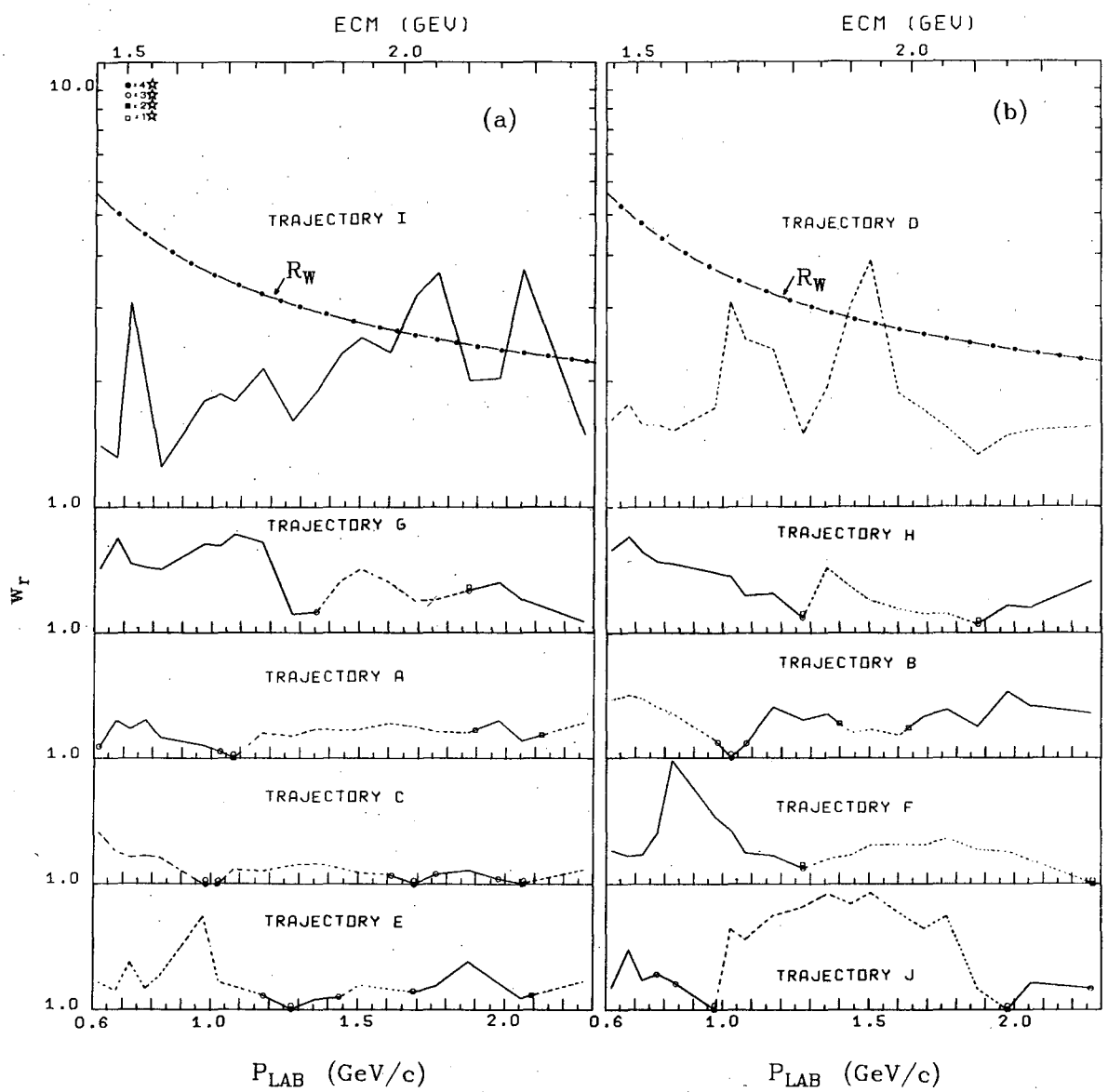

XBL 777-1448

Figure 33

This report was done with support from the Department of Energy. Any conclusions or opinions expressed in this report represent solely those of the author(s) and not necessarily those of The Regents of the University of California, the Lawrence Berkeley Laboratory or the Department of Energy.

TECHNICAL INFORMATION DEPARTMENT
LAWRENCE BERKELEY LABORATORY
UNIVERSITY OF CALIFORNIA
BERKELEY, CALIFORNIA 94720